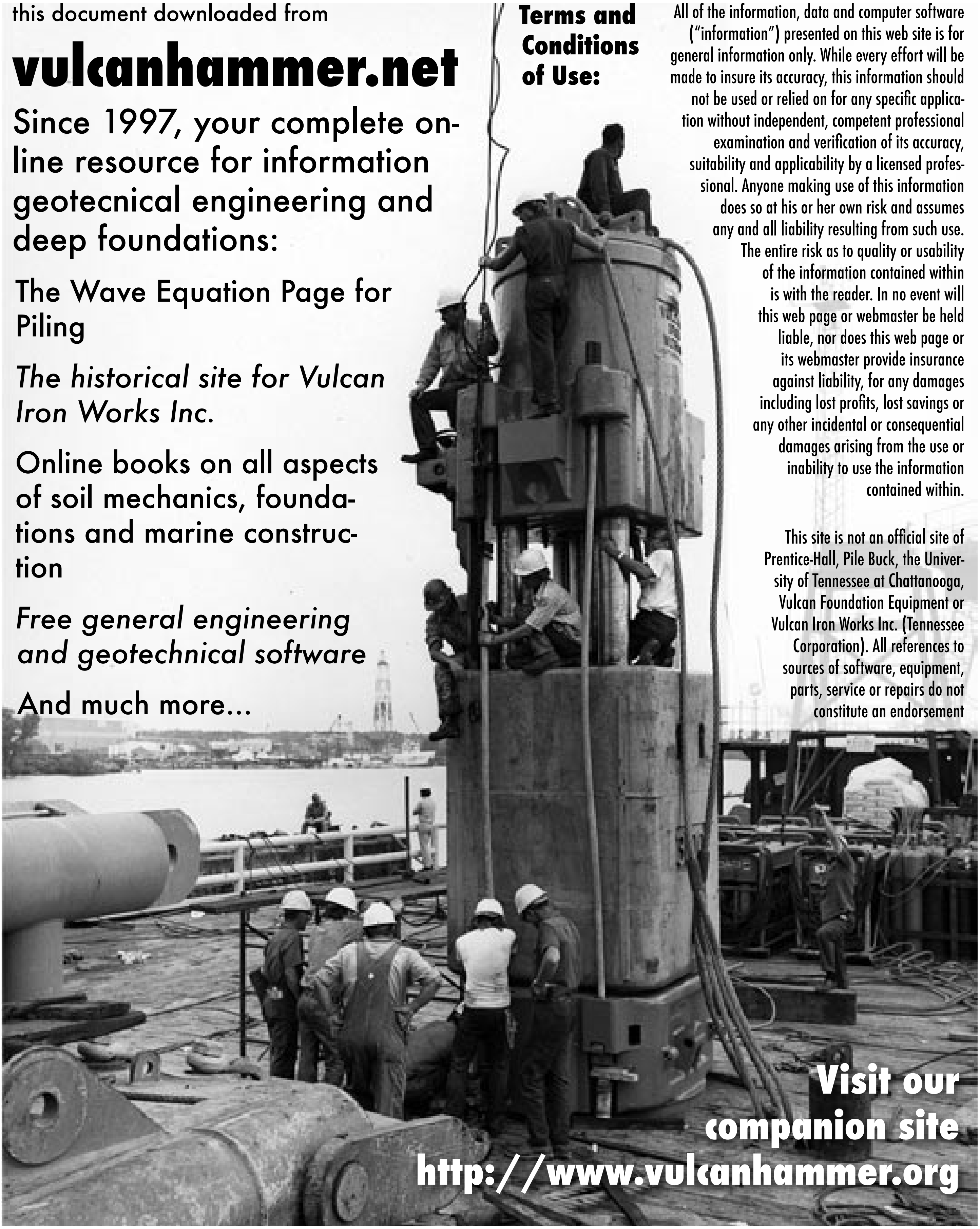

SOIL MOTIONS UNDER VIBRATING FOUNDATIONS

A Dissertation

By

JOHN VIVIAN PERRY, JR.

Submitted to the Graduate School of the
Agricultural and Mechanical College of Texas in
partial fulfillment of the requirements for the degree of

DOCTOR OF PHILOSOPHY

August 1963

Major Subject Mechanical Engineering

SOIL MOTIONS UNDER VIBRATING FOUNDATIONS

A Dissertation

By

JOHN VIVIAN PERRY, JR.

Approved as to style and content by:

R. M. Wingren
(Chairman of Committee)

C M Simmons
(Head of Department)

August 1963

ABSTRACT

Soil Motions under Vibrating Foundations

John V. Perry, Jr., B.S., Virginia Polytechnic Institute

M.S., Texas A & M University

Directed by: Prof. Spencer J. Buchanan

and Prof. Roy M. Wingren

This research was undertaken to determine the amount and extent of soil motions under vibrating foundations. The test soil was standard 20-30 Ottawa sand, ASTM C-190, that was contained in a one-meter cubical box. A force generator was mounted above the soil and applied dynamic loads to a circular footing. These were harmonic forces and were applied at frequencies between five and fifty cycles per second.

Three hundred and sixty-seven test runs were recorded on an electromagnetic oscillograph from signals generated by an accelerometer buried in the soil. This accelerometer was located at various depths beneath the center of a footing and, at other times, it was located beneath and offcenter. Other variables were the footings which had different diameters and masses.

Three empirical equations were developed from the test results using dimensional analysis. These equations were for maximum values of acceleration, velocity and displacement, respectively.

ACKNOWLEDGMENTS

My sincere regards go to Dean W. C. Hall, Dean F. J. Benson and Dr. C. M. Simmang for their interests, considerations and financial aid that made possible this investigation.

Deep appreciation is extended to the members of my committee: Professors C. W. Crawford, L. S. O'Bannon and R. M. Wingren - Mechanical Engineering Department; Dr. R. E. Basye - Mathematics; Professor S. J. Buchanan - Civil Engineering Department; and Dr. H. T. Kennedy - Petroleum Engineering Department; for their confidence, guidance, and counseling.

My associates: S. E. Brown, J. R. Carter, R. H. Gibson, J. G. Simek, H. G. Stallings, and Hoyett Taylor are recognized for their contributions toward the design, manufacture, and construction of the vibrator, foundation and electronic components.

Special thanks are given Professor A. M. Gaddis for technical assistance in the instrumentation of the project, also Professor L. S. O'Bannon for his many helpful suggestions and friendship over the years.

Restitution can never be made to my wife, Helen, and my children, John, Judy and Joan, for what they have endured, but their sacrifices have been both noticed and appreciated.

TABLE OF CONTENTS

LIST OF TABLES

LIST OF FIGURES

LIST OF SYMBOLS

Symbol		Dimensions
A_d	Double amplitude of light beam trace from accelerometer	L
A'_d	Double amplitude of light beam trace from accelerometer during calibration	L
C_c	Calibration curves	none
D_d	Relative density of sand	none
D_f	Foundation diameter	L
E	Accelerometer sensitivity	F
E_c	Calibrated accelerometer sensitivity	F
F	Dimension of force	F
F_m	Mean force applied to the sand	F
F_v	Variable harmonic force applied to the sand	F
F_1	Minimum force sensed by the transducer	F
F_2	Maximum force sensed by the transducer	F
G	Specific gravity of solids in sand	none
H	Depth of free sand in box	L
H_b	Depth of sand under the foundation	L
L	Dimension of length	L
R	Horizontal distance between foundation and accelerometer centers	L
S	Foundation settlement	L
T	Dimension of time	T
V	Volume of solids, air and water in sand	L^3
W	Weight (mass) of sand in box	$FL^{-1}T^2$

Symbol		Dimensions
W_a	Weight (mass) of foundation elements above transducer	$FL^{-1}T^2$
W_b	Weight (mass) of transducer and foundation elements below transducer	$FL^{-1}T^2$
W_f	Weight (mass) of foundation	$FL^{-1}T^2$
W_s	Dry weight (mass) of sand	$FL^{-1}T^2$
Y	Vertical distance between bottom of foundation and top of accelerometer	L
e	Void ratio of sand	none
f	Frequency	T^{-1}
g	Local acceleration due to gravity	LT^{-2}
k	Spring rate	FL^{-1}
m_f	Mass of foundation	$FL^{-1}T^2$
r	Ratio = Y/D_f	none
r_o	Foundation radius	L
w	Moisture content of sand	none
γ_w	Unit weight of water	FL^{-3}
δ	Amplitude	L
$\dot{\delta}$	Maximum velocity	LT^{-1}
$\ddot{\delta}$	Maximum acceleration	LT^{-2}
δ_d	Double amplitude	L
$\ddot{\delta}_o$	Acceleration at $Y = 0$	LT^{-2}
$\ddot{\delta}_r$	Acceleration at r	LT^{-2}
ρ	Sand density	FL^{-3}
μ	One millionth, micro	none

CHAPTER I

INTRODUCTION

The purpose of this investigation was to determine the steady state soil motions under circular footings when acted upon by harmonically applied forces. The results in Chapter IV were obtained using the test facility and procedure described in Chapters II and III.

The author has been interested for some time in the study of vibrations and soil mechanics. He and his associates have acted as consultants on foundation vibrations problems and are concerned with the inadequacy of knowledge that would enable engineers to design a soil-foundation system with confidence. The soil-foundation system refers to the machine, the structure connecting it to the foundation, the foundation and the supporting soil.

The vibrations of this system can be determined in many ways once the installation has been made. However, no acceptable method has been found to design accurately the system, such that its vibrations can be predicted before installation. The unknown influence that some factors have on a particular system preclude an accurate design. Such factors are the kind, condition and arrangement of the soil. Also, the same factors vary with depth, location and environment.

Numerous investigations(1)*, both empirical and theoretical, have been made to resolve the factors which influence the vibrations of a soil-foundation system. One of the theoretical approaches to the problem(2) assumes the mass of soil, which vibrates with a foundation, is that contained in a right circular cylinder of the elastic half-space having a radius r_o and a height r_o/π. One purpose of this investigation was to test the validity of this assumption.

* Numbers in parentheses refer to references at the end of this dissertation.

CHAPTER II

EQUIPMENT

The experimental equipment is shown in Figures 1 through 16 and was located in the Mechanical Engineering Analog Computer Laboratory. One item not shown, a vacuum tube voltmeter borrowed from the Electrical Engineering Department, was used to check the output of the microvolter (Figures 2 and 13).

Recording Equipment

The oscillograph(3) records variable electric currents by the use of electromagnetic galvanometers in conjunction with a light source and a moving strip of photographic paper. Its timing system consists of a motor, slotted disk, fork, and light which records time lines (Figure 20) at 0.01 second intervals. The photographic paper speed may be varied from approximately 4 to 50 inches per second. This paper is available in 6 inch widths and either 100 or 200 foot rolls. The recording switch has OFF, AUTOMATIC, and MANUAL positions. A recording continued as long as the manual switch was held closed and for a 2 foot record with the automatic switch closed. A footage counter indicated the amount of paper used and a numbering counter projected a number (Figure 20) on each record. The sensitivity of the oscillograph was limited to that of the galvanometers and is inversely proportional to the square of the galvanometer natural frequency.

Calibration Equipment

The accelerometer calibration equipment included the oscillator, microvolter and tee-box (Figures 2, 13 and 14). The oscillator introduced a preset frequency into the system; the microvolter, a preset voltage; and the tee-box enabled the system to be switched in or out. The force transducer and load springs had calibration equipment (Figures 3, 4, 5 and 13) composed of a strain gage indicator, loading rod, and known weights. A strobotac was used to set the frequency of loading.

Other Equipment

The entire system was so designed that many variations of D_f, F_m, F_v, f, H, m_f, R, and Y could be made. Additional mass could be added to the foundation by using the pressure gage calibration weights in the mechanical laboratory.

<u>Transducers</u>. The force transducer(4, 5, 6) Figure 16) has four strain gages bonded at ninety-degree intervals around the middle. Each gage has a factor of 2.08 and a resistance of 120 ohms $\pm$ 2%. The transducer is a part of the foundation (Figure 12).

The accelerometer(7), shown hanging on a nail inside the box in Figures 7, 8, and 9, is a piezoelectric device with a stainless steel case 0.60 inches in diameter by 0.42 inches thick and weighs 11 grams with mounting screw.

Amplifier. The amplifier(8) (Figure 2) has a selector switch with settings of 1, 3 and 10 gains; an input selector switch with the second of three positions recommended for use with all piezoelectric and capacitive type pickups; and an output standardizer that makes it possible to standardize the sensitivity of any accelerometer to a value E less than its original calibration E_c. The amplifier is energized by the power supply (Figure 15) which includes a transformer(9) for low frequency response.

Soil, container and beam. The soil tested was standard 20-30 Ottawa sand(10, 11, 12). It was obtained in seventy 50 pound bags (Figure 6). A one-meter cubical box, inside dimensions, was the container in which the sand was placed for testing. The box (Figures 3, 4 and 7 through 11) was constructed of one-half inch plywood, reinforced with 2" x 4" lumber and had metal bearing plates around the top periphery. These plates supported the depth gage and loading beam (Figures 10 and 11). The loading beam was a 6-inch, wide-flange, 25 pounds per foot steel beam. Mounted on this beam were the loading frame and variable speed drive (Figures 10 and 11). The beam, variable speed drive and loading frame were mounted such that the load point (Figure 7) could be positioned at any place inside the box.

Loading frame and foundation. The loading frame (Figures 5 and 7 through 11) was fabricated by welding various steel sections and had bolted to it two Sealmaster ball bearings No. SFT-12. These self aligning bearings supported the three-quarter inch diameter shaft, 13 inches long, that had a V-pulley keyed to one end and an eccentric machined on the other. The eccentric has a New Departure bearing No. 77-R-6 pressed on and held from axial movement by an Industrial retaining ring No. 3100-37. There are two such shafts, one has an eccentricity of 0.167 inches and the other half that. The shaft is belt driven from the Reeves Vari-Speed Motordrive, "C" Flow, 100-1A-12, having output speeds from 310 to 3100 revolutions per minute.

The loading frame front flanges have two holes, each is one-half inch in diameter, drilled three and seven-eights inches on centers. Through these holes are inserted steel rods of adequate hardness. The rods had a diameter of 0.4990 inches with tolerances of $^{+0.0000}_{-0.0005}$ inches. An aluminum follower was machined to hold one, two or three Briggs and Stratton exhaust valve springs No. 26478 and two Thompson ball bushings No. A-81420. The top of the follower has a Conolite bearing plate cemented to the center. This plate makes contact with the bearing on the shaft eccentric. The bushings, held in place in the follower with two Industrial retaining rings No. 3100-87, allowed the follower to move freely on the steel rods.

Beneath the follower and separated by the springs is the loading bar with adapter (Figure 12). This bar is machined similarly to the follower and has its adapter screwed to the bottom. The adapter has a hole for inserting a plumb bob string and one end has a cone-shaped depression to hold the column adapter.

The column (Figure 12) rested on a steel loading plate that was screwed to the foundation disk. Seven disks were made; one had a ten square centimeter area; and the others had diameters of 4, 5, 6, 6.28, 7, and 10 inches. The length of the foundation elements could be varied by screwing the threaded rod inside the column and securing them with a locking nut. There were three sets of these steel columns and rods; long, intermediate and short.

<u>Depth gages</u>. The depth gages were vertical 1" x 4" S4S boards secured to a horizontal screed (Figures 7 through 9) at their lower ends. The verticals (Figures 10 and 11) passed through brackets and were held in place with set screws. The depth of sand in the box could be read on meter scales at indexes on the brackets. The scales were cut from a meter stick and glued to rabbeting in each vertical. This device also served to level the sand in the box. Depths were read to whole millimeters and estimated to fractions of a millimeter.

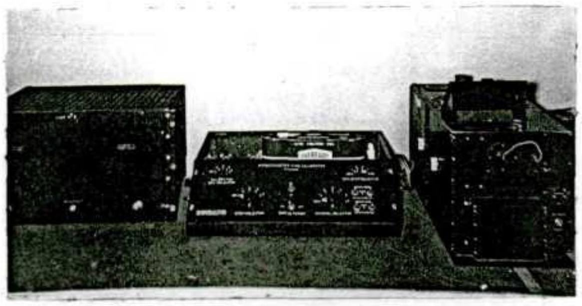

Figure 1. Recording equipment and potentiometer type calibrator.

Figure 2. Calibration and accelerometer amplifying equipment.

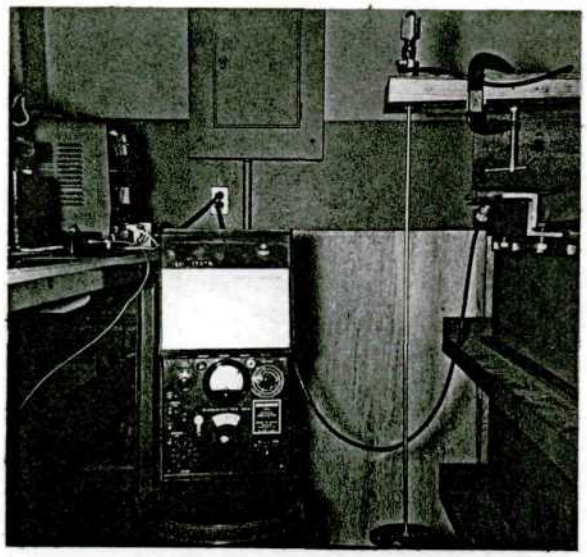

Figure 3. Calibration position for force transducer with loading rod and indicator.

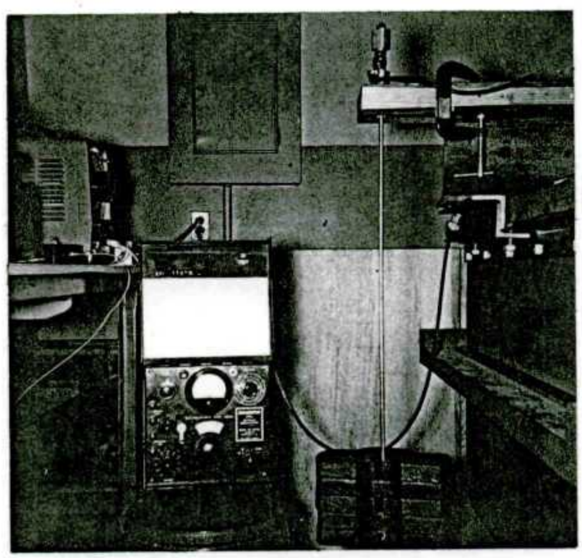

Figure 4. Calibration position for force transducer with loading rod, five ten-pound weights, and indicator.

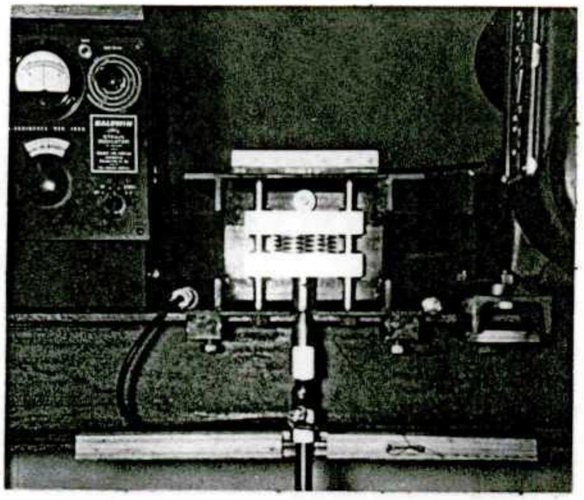

Figure 5. Three loading springs in calibration position with indicator and force transducer.

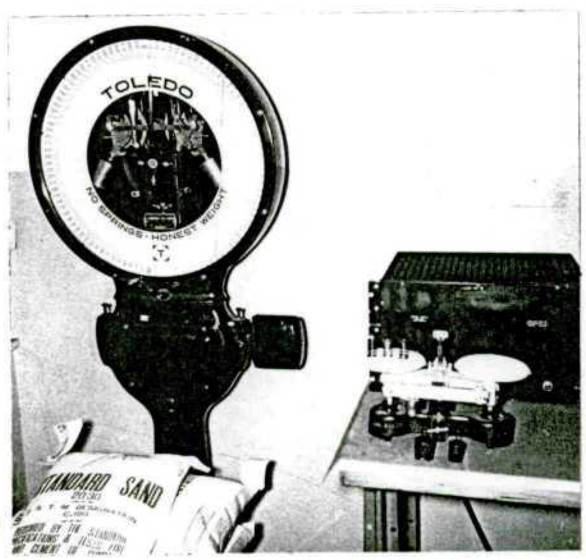

Figure 6. Scales for weighing sand and balance for small equipment.

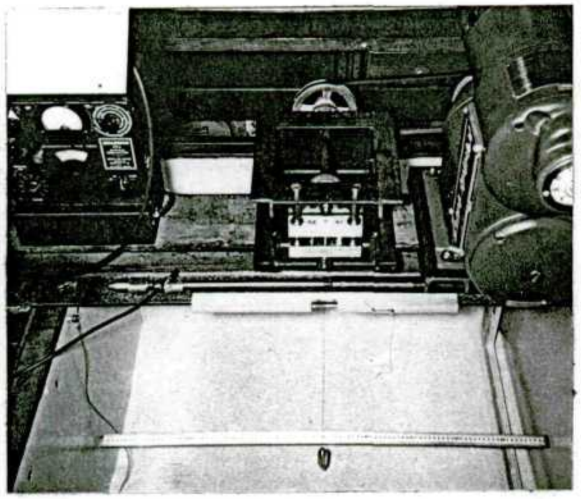

Figure 7. Centered load point.

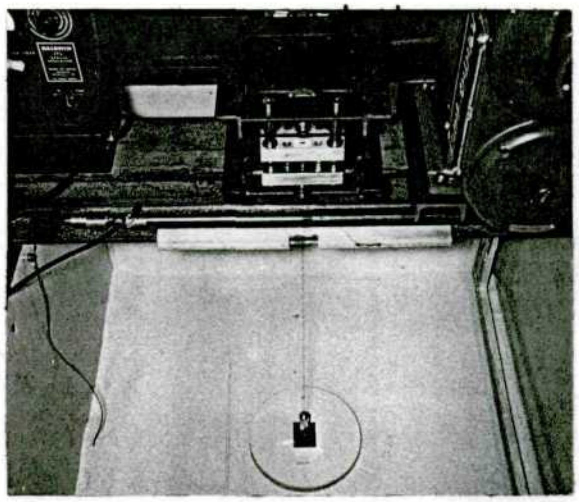

Figure 8. Foundation aligned under load point.

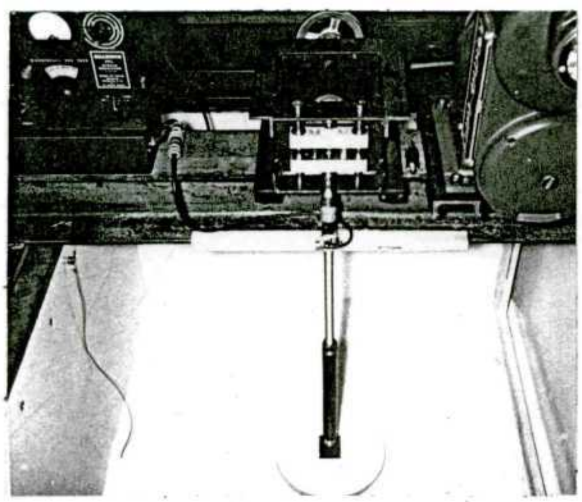

Figure 9. Loading column in position.

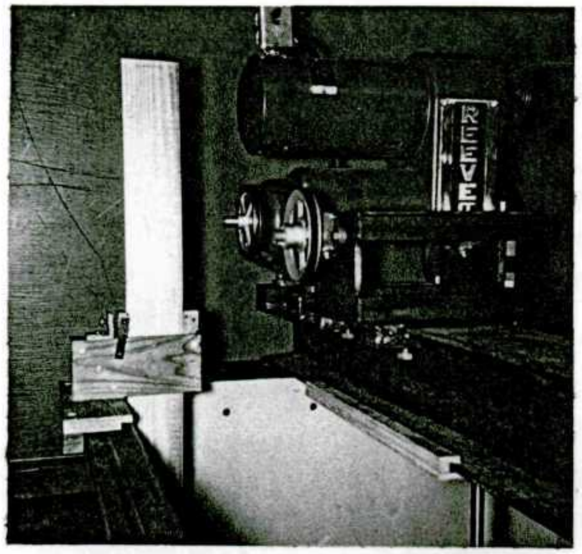

Figure 10. Left depth gage and belt transmission between variable speed drive and loading frame.

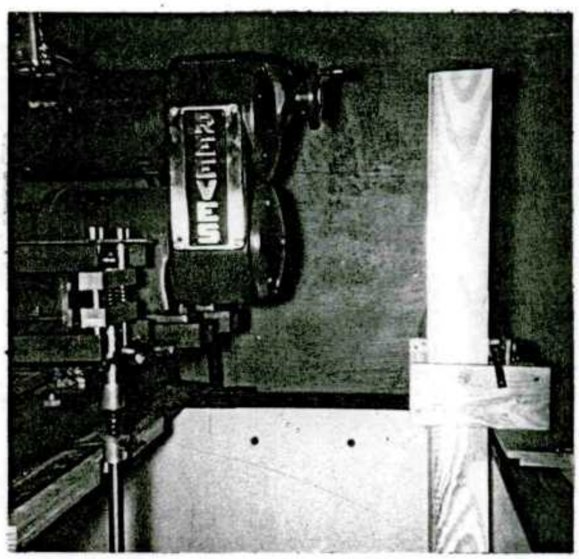

Figure 11. Drive side of loading frame and right depth gage.

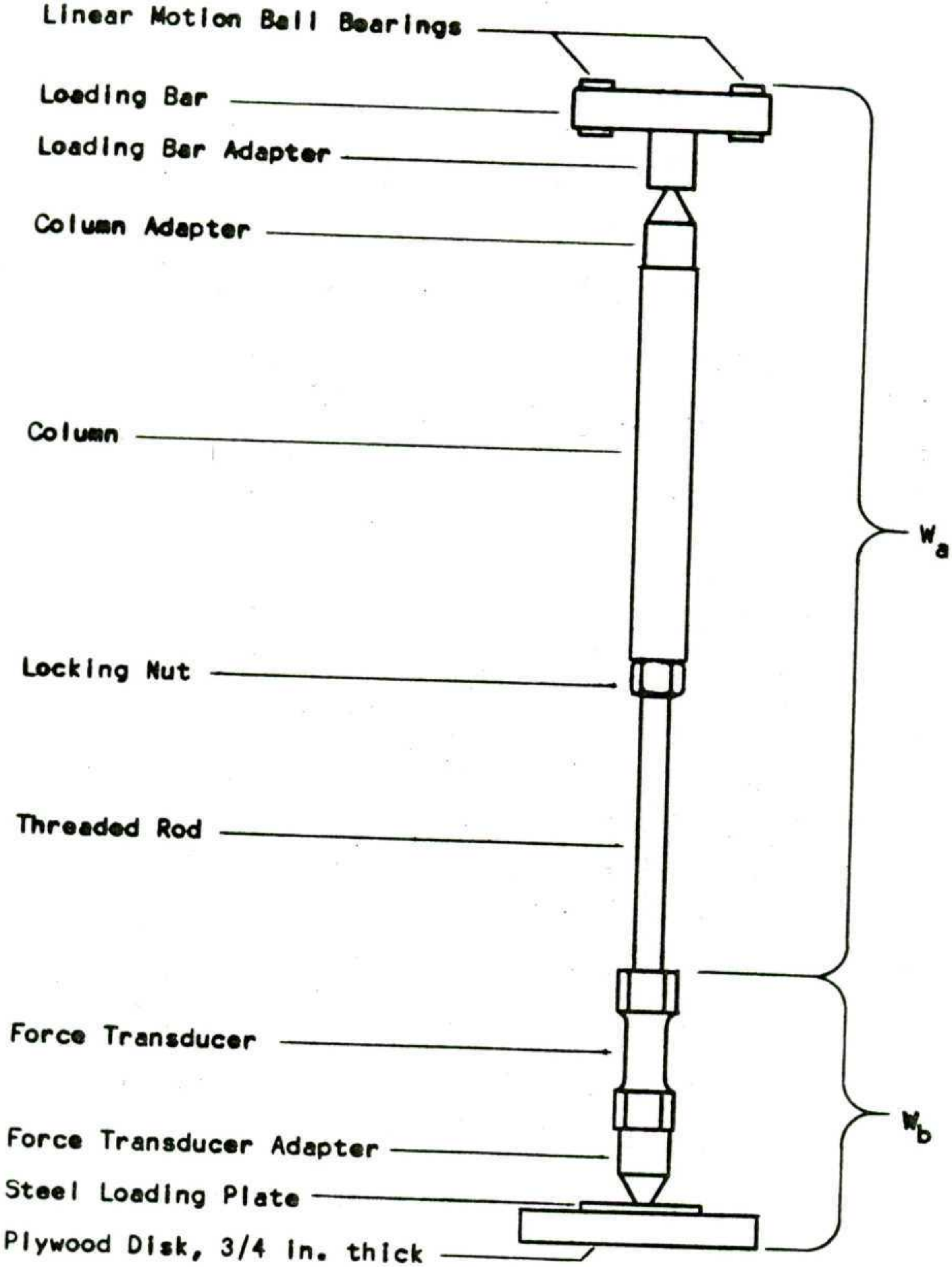

Figure 12. Elements included in the foundation..

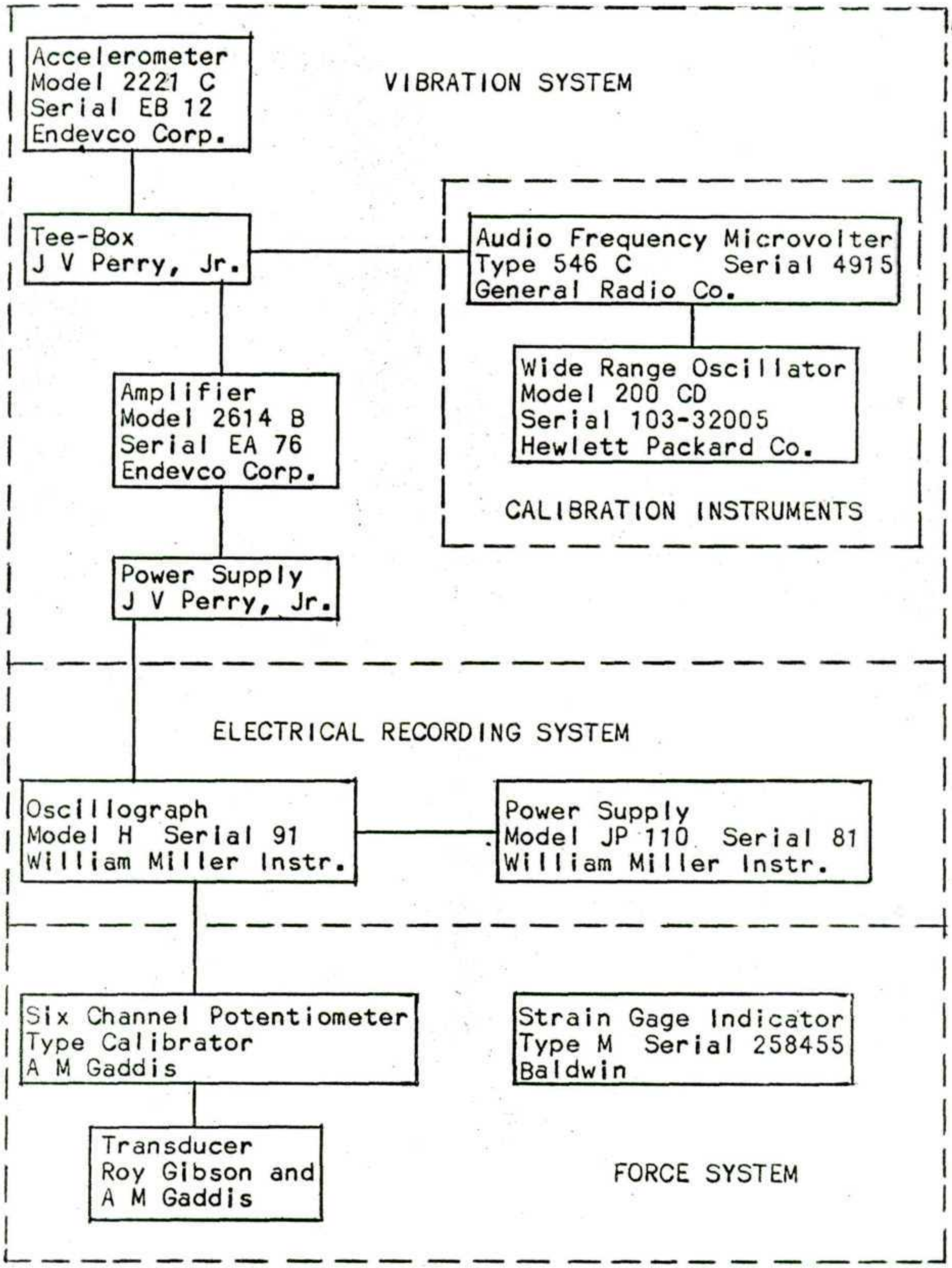

Figure 13. Electrical equipment configuration.

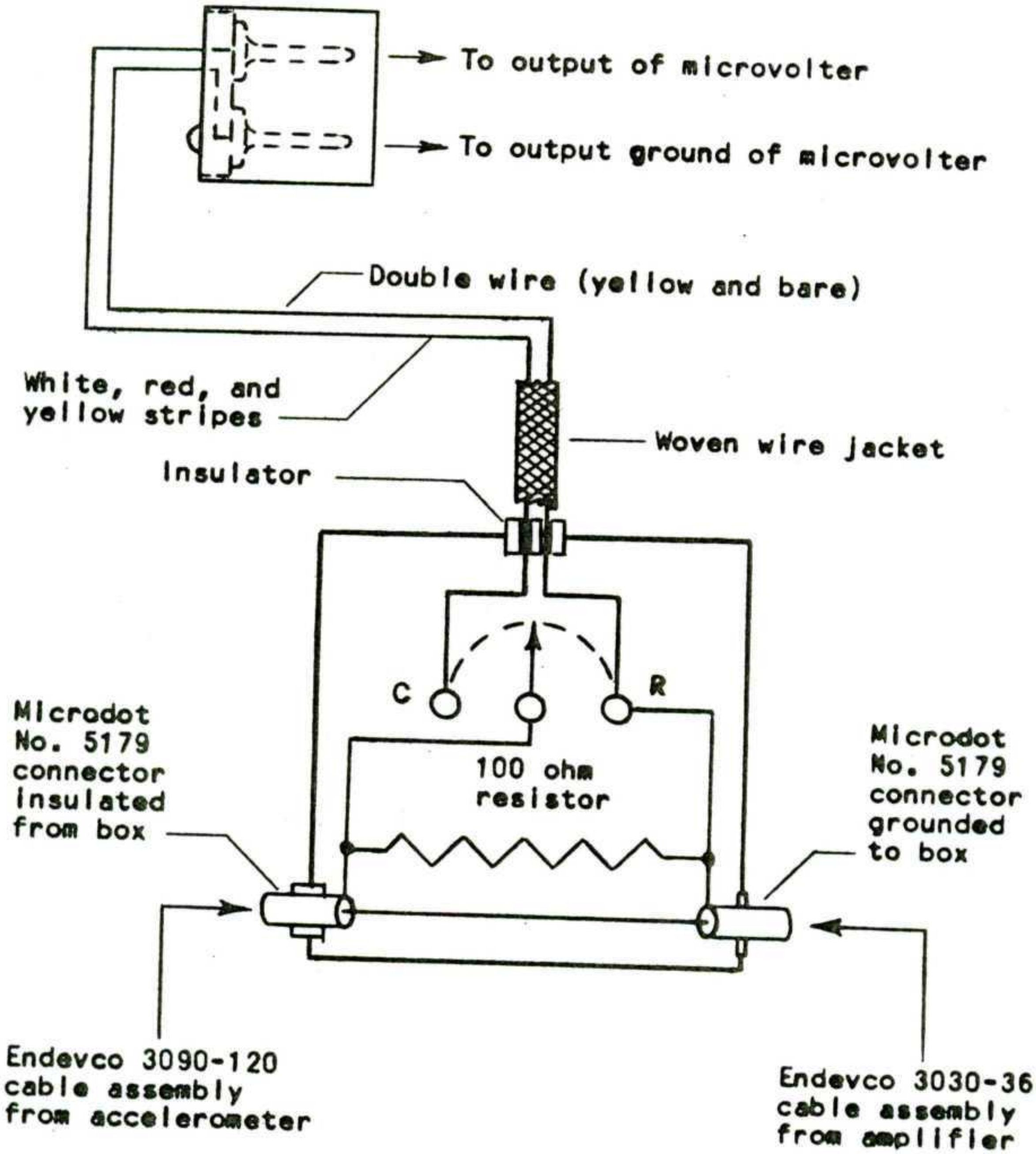

Notes:
1. C is the switch position for calibrate.
2. R is the switch position for run.
3. Not to scale.

Figure 14. Tee-box and connectors.

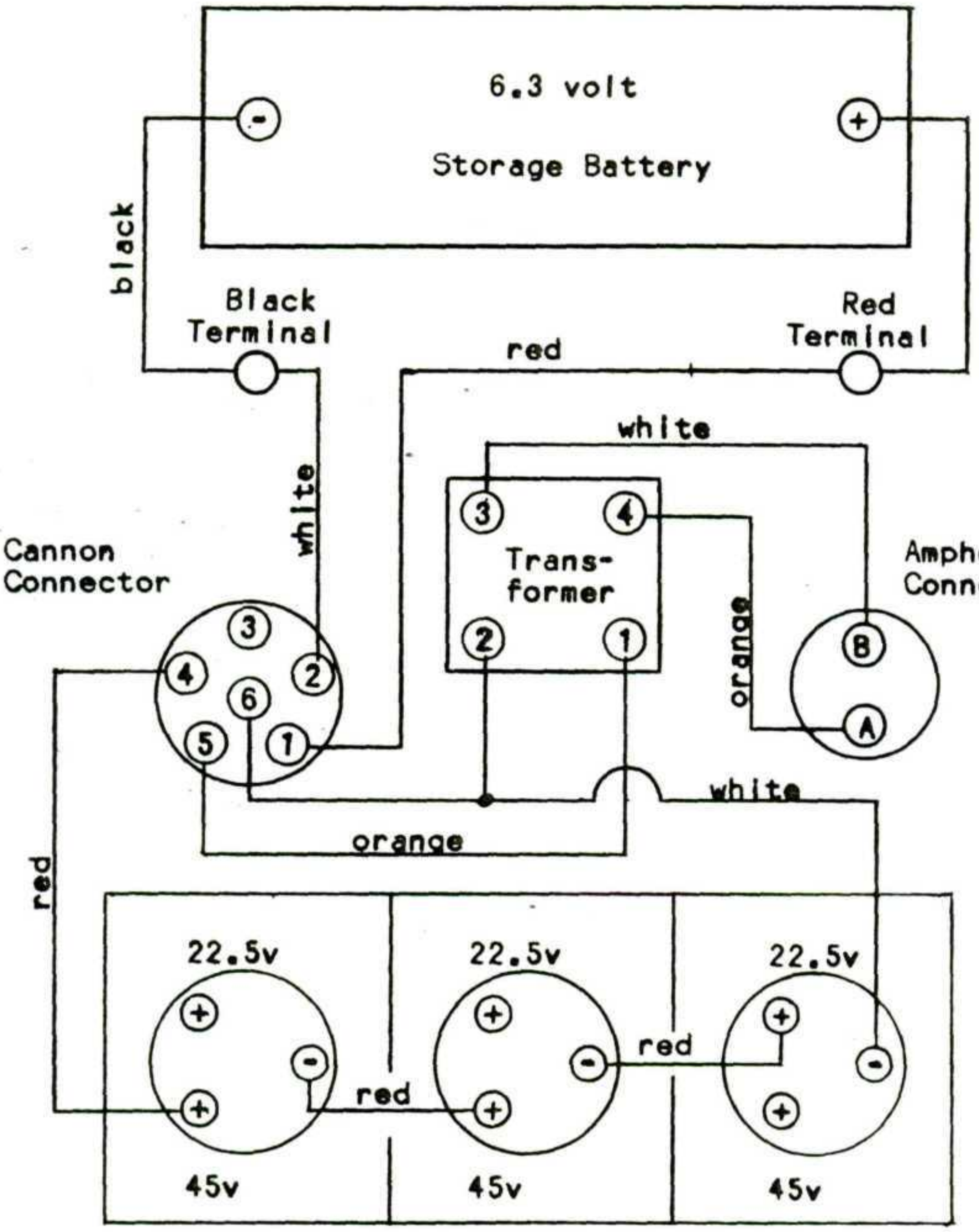

Notes: 1. Cannon RWK-6-31SL mates with RWK-6-22C-1/4 on cable. The other end of cable has WK-6-21C-1/4 that mates with WK-6-32S on Endevco amplifier.

2. Amphenol AN-3102-A-10SL-4P mates with AN-3106-A-10SL-4S (C).

3. Transformer is Endevco model 2609.1.

Figure 15. Amplifier power supply.

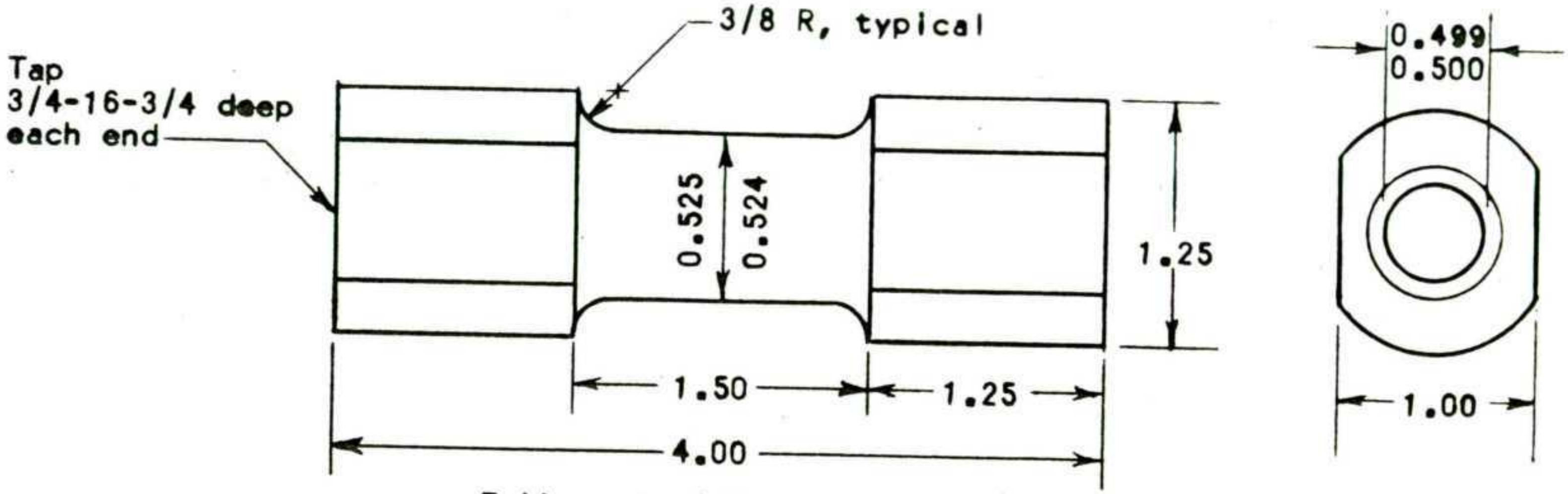

Full scale (dimensions in inches)

Material: 2024 - T4, Aluminum

Mechanical properties:

68,000 psi = ultimate strength in tension

47,000 psi = yield strength in tension

41,000 psi = ultimate strength in shear

20,000 psi = endurance strength in reversed bending at 5×10^8 cycles

10.6×10^6 psi = modulus of elasticity (average of tension and compression)

Physical properties:

0.10 lb_m / $inch^3$ = specific weight

935°F - 1180°F = melting range

Figure 16. Force transducer without strain gages.

CHAPTER III

PROCEDURE

This chapter is subdivided into assumptions and procedure. The assumptions apply to the soil and the procedure includes equipment calibration and method of testing. The results are given in Chapter IV.

Assumptions

The kind and arrangement of the soil were constants. Other constants were; $w = 0.115\%$, and $G = 2.75$. The relative density(11 and 14) was a variable and its effect was minimized by loading the foundation at six dial settings (Figure 17) of the variable speed drive, viz. 1, 3, 5, 6, 7, and 8. This gave full settlement to the foundation before the record runs were made.

The relative density, $D_d = (e_{max} - e)/(e_{max} - e_{min})$, where $e = (G\gamma_w V/W_s) - 1$, was not held constant because of variations in V/W_s. The isopyc(15) and value of V/W_s would be difficult to determine since the zone(16) that bounds V depends upon the initial density and the periodic impulses from the vibrator. According to R. K. Bernhard and J. Finelli (page 252 of reference 1) it is difficult to measure density variations with soil depth.

The coefficient of dynamic subgrade reaction(17) was another variable that was neglected. This coefficient depends, in part, upon the size and shape of the loaded area.

Procedure

Calibration of equipment. The force gage was positioned for compression (Figures 3 and 4) and found to have a straight line relationship between deflection and load up to the maximum expected load of 100 pounds. The springs were checked against the force gage (Figure 5) to find the spring rate and the F_v which could be applied with one, two and three springs. This information is in Appendix A.

The accelerometer had a factory calibration but this did not go below 20 cycles per second, cps. Therefore, the accelerometer was calibrated between f = 5 cps and 20 cps as follows:

1. The accelerometer was screwed to the top of the follower which had a $\delta_d = 0.334$ inches.

2. The follower was vibrated at a known frequency and A_d measured.

3. The value of $\ddot{\delta}/g$ was calculated using the relation $(\delta_d/2)(2\pi f)^2/g$, and A_d' was obtained for this frequency and recording equipment configuration from $A_d/(\ddot{\delta}/g)g$ equals $A_d'/(0.10g)$.

4. Steps 2 and 3 were repeated using different frequencies and a graph made of $A_d'/(0.10g)$ versus f. Values of A_d' were taken from this graph at f = 5, 10, 15 and 20 cps.

5. A frequency of 5 cps was set on the oscillator and the microvolter adjusted to give the same A_d' at this

frequency from the graph in step 4. This voltage was the equivalent of 0.10g for f = 5 cps.

6. Step 5 was repeated at frequencies of 10, 15, and 20 cps.

The accelerometer and recording equipment calibration was accomplished for the runs as follows:

1. A voltage, equivalent to 1g, was set on the microvolter and f = 5 cps was set on the oscillator. These signals were sent through the system and a record taken on the oscillograph paper.

2. The frequency was changed in increments of 5 cps extending over the range and records taken of each.

3. Steps 1 and 2 were repeated for voltage equivalents of 0.50g and 0.10g.

Typical records are shown as a set in Figure 18. The equipment was calibrated before, during, and after a series of runs and averaged to obtain the proper curve. These curves are shown in Figure 19 and the corresponding runs in Table 6. Appendix B has the factory calibration information.

The Reeves Vari-Drive did not need calibrating but a performance curve (Figure 17) was drawn to find the output speed for a particular dial setting. This curve helped to obtain a value close to the desired frequency by setting the dial.

The potentiometer type calibrator (Figure 1) was adjusted to give a one inch deviation from the zero force line (Figure 20) for each twenty pounds of force.

Method of testing. Bags of sand were weighed (Figure 6), and the sand poured into the box. The empty bags were then weighed to determine the sand weight. The sand top surface was screeded level and its depth measured with the depth gage. This is recorded in Appendix C and averaged 36.71 pounds per centimeter of depth.

The beam, vari-drive, and loading frame were adjusted and locked in position with load point centered in the box (Figure 7). The accelerometer was positioned at a known location for each run. Four methods were used to bury the accelerometer in the sand:

1. An insulated steel rod, 38 cm long, was positioned vertically and supported by the box and sand. The accelerometer was placed over the rod so that its top surface was flush with the upper end of the rod.

2. It was supported only by the sand.

3. It was placed on top a piece of filter paper 11 cm in diameter.

4. It was screwed to a thin aluminum disk 3 in. in diameter.

Refer to Appendix D for information regarding each run.

A foundation was aligned under load point (Figure 8), and loading column placed in position (Figure 9). The elements included in the foundation were actually positioned with the force transducer near the bottom (Figure 12). This allowed the transducer to sense all forces transferred to the soil except those coming from the transducer, its adapter, steel loading plate and plywood disk. The weights of all foundation elements, springs, and follower are in Appendix C.

The record runs were made using different foundation diameters and masses, and at various values of Y, R, F_m, F_v, and f. Approximately 900 runs were made but only 367 (Tables 1 through 4) were used. The ones not used showed little or no accelerometer excitation as seen in Figure 21 for Run No. 157.

Information from a photographic record for Run No. 291 is shown in Figure 20. The top curve is from the accelerometer system and its jaggedness illustrates noise. Values taken from the record are recorded in Table 4; A'_d is from the appropriate calibration curve in Figure 19 and Table 6. The determination of F_m for this run and W_f for runs 1 through 18 and 19 through 42 are in Appendix E.

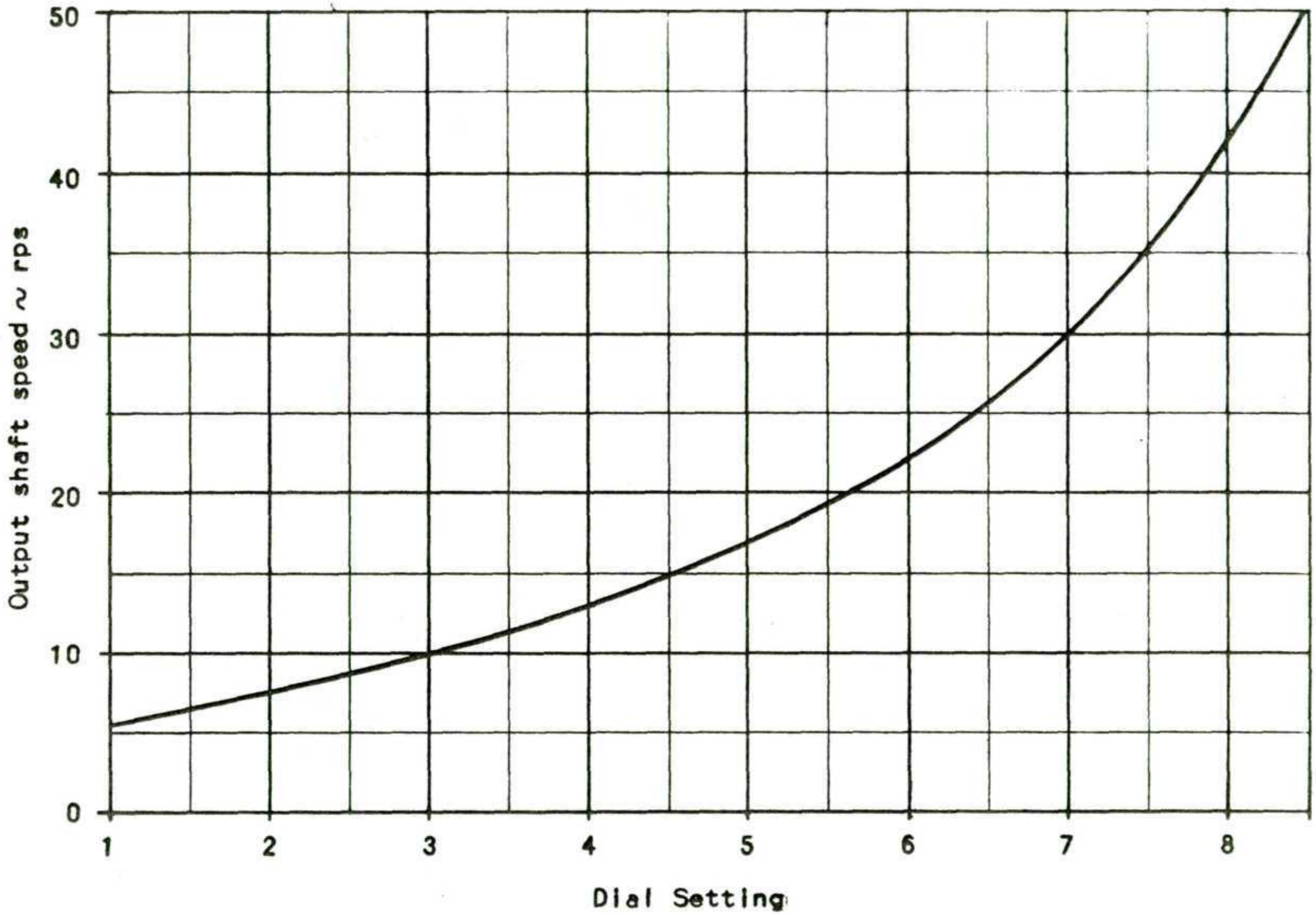

Figure 17. Performance curve of Reeves Vari-Speed Motordrive.

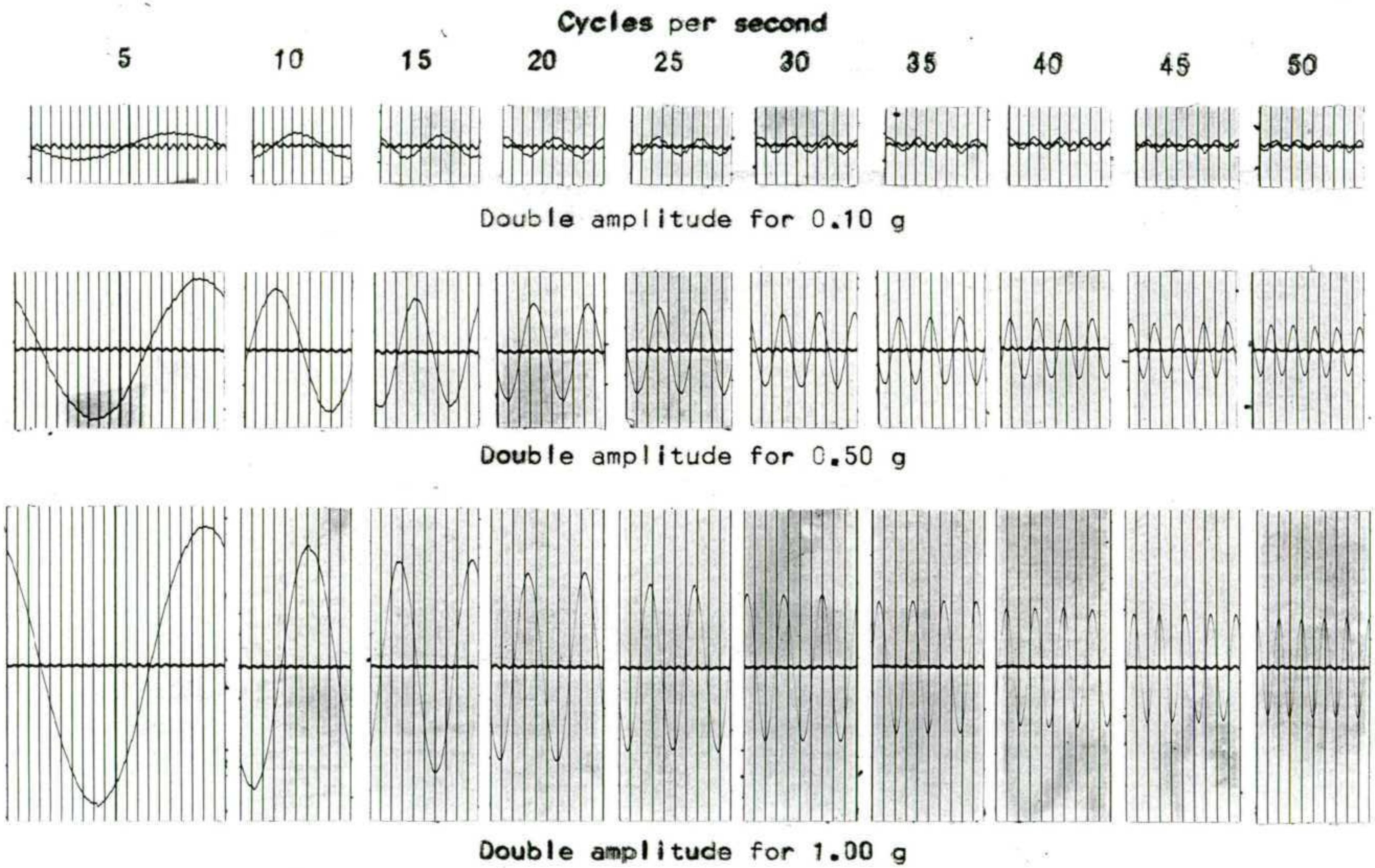

Figure 18. Accelerometer and recording equipment calibration records (full size).

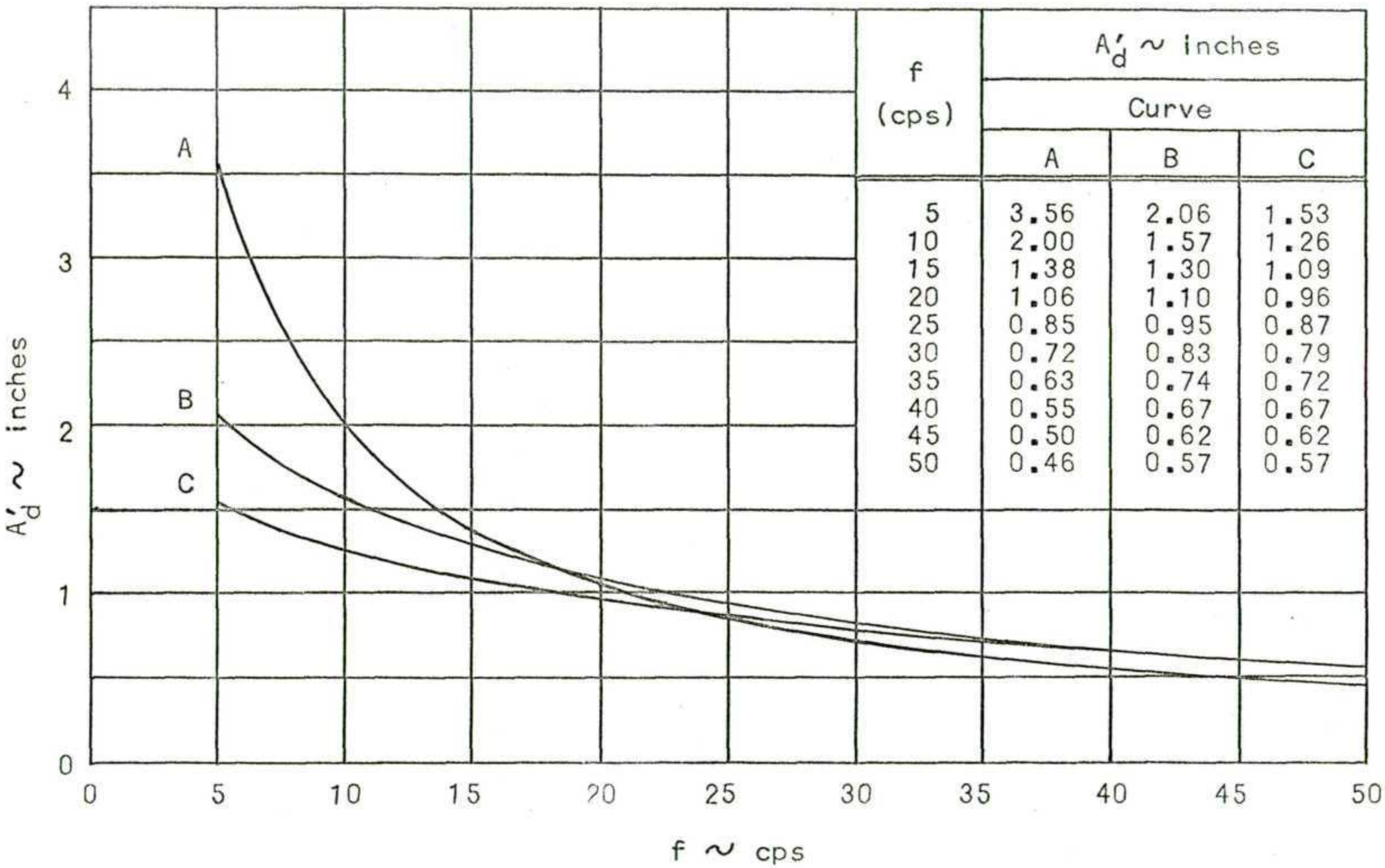

f (cps)	A'_d ~ inches Curve A	B	C
5	3.56	2.06	1.53
10	2.00	1.57	1.26
15	1.38	1.30	1.09
20	1.06	1.10	0.96
25	0.85	0.95	0.87
30	0.72	0.83	0.79
35	0.63	0.74	0.72
40	0.55	0.67	0.67
45	0.50	0.62	0.62
50	0.46	0.57	0.57

Figure 19. Accelerometer and recording equipment calibration curves for 0.10 g.

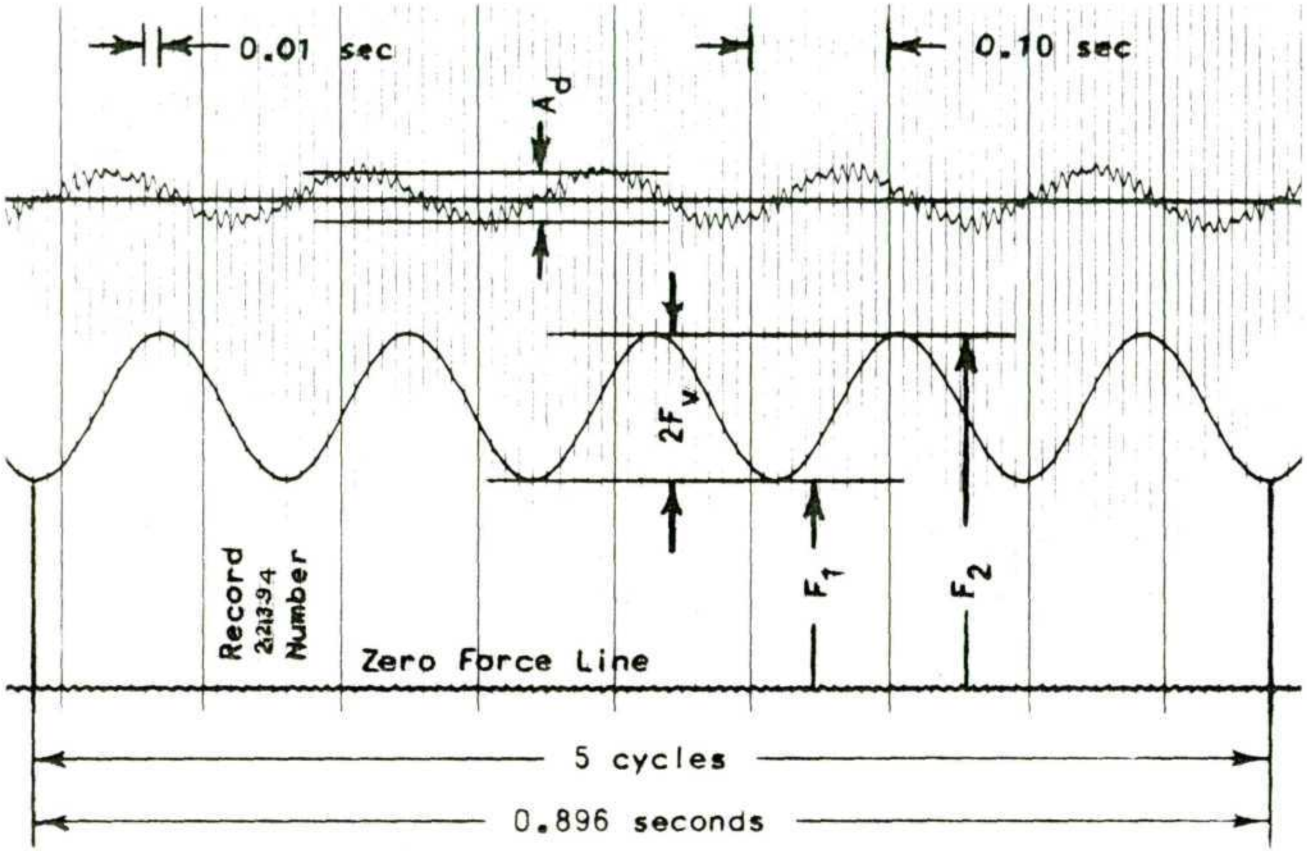

Record No. 22394	This is for	F_1 = 21.6 lb_f
A_d = 0.26 in.	Run No. 291	F_2 = 36.8 lb_f
f = 5.58 cps		F_v = 7.6 lb_f

Figure 20. Information obtained from photographic record.

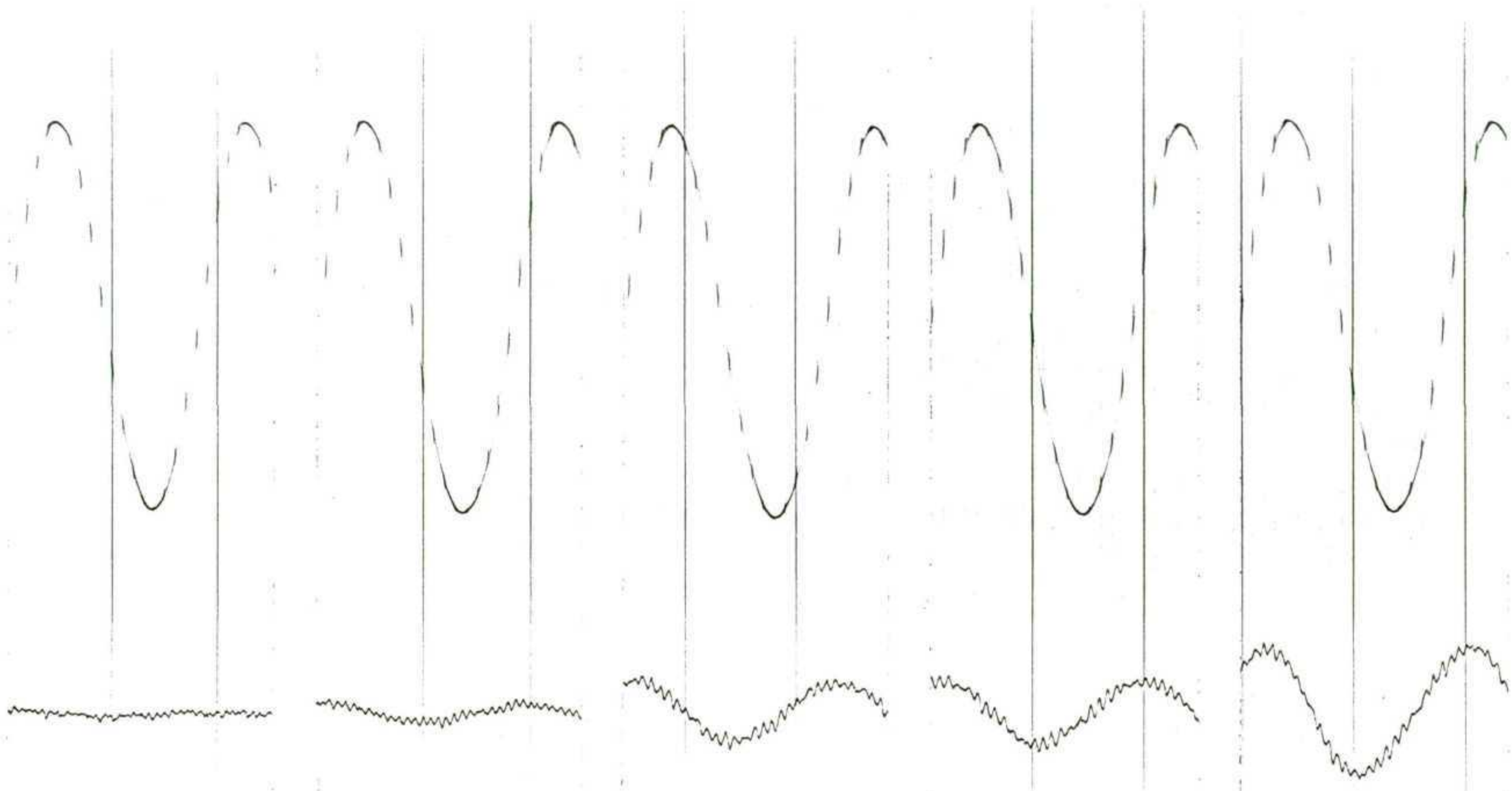

Run No. 157 Y = 8.40 in.

Run No. 159 Y = 4.52 in.

Run No. 161 Y = 1.97 in.

Run No. 163 Y = 1.18 in.

Run No. 165 Y = 0.39 in.

Figure 21. Five photographs showing changes in accelerometer output as (Y) decreases.

CHAPTER IV

RESULTS

The results are given in Tables 1 through 4. The columns headed $\dot{\delta}$ and δ_d were completed using the values for f and $\ddot{\delta}/g$ with a vibration nomograph (Figure 22). Table 5 contains information on settlements and Table 6 shows the calibration curve and run correspondence. Dimensionless parameters(13) are shown in Table 7 for some of the runs and presented graphically in Figure 23. From this figure, equations are written as follows:

$$\ddot{\delta}_o = 0.036\ f(D_f F_v/m_f)^{0.5} \qquad [1]$$

$$\ddot{\delta}_{0.37} = 0.010\ f(D_f F_v/m_f)^{0.5} \qquad [2]$$

$$\ddot{\delta}_{0.78} = 0.006\ f(D_f F_v/m_f)^{0.5} \qquad [3]$$

$$\ddot{\delta}_{1.38} = 0.0033\ f(D_f F_v/m_f)^{0.5} \qquad [4]$$

$$\ddot{\delta}_{0.37}/\ddot{\delta}_o = 0.278 \qquad [5]$$

$$\ddot{\delta}_{0.78}/\ddot{\delta}_o = 0.167 \qquad [6]$$

$$\ddot{\delta}_{1.38}/\ddot{\delta}_o = 0.092 \qquad [7]$$

The last three equations are shown graphically in Figure 24 as the dotted line. An approximate equation for this line is:

$$\ddot{\delta}_r/\ddot{\delta}_o = (0.032)^r \qquad [8],$$

shown as the solid curve in the figure.

For Run No. 157, values of f, D_f, F_v, and m_f were put into Eq. [1] and give $\ddot{\delta}_o$ = 18.6 in. per sec^2. The experimental result of $\ddot{\delta}_r$ = 0.773 in. per sec^2 at r = 1.34. The corresponding value of $\ddot{\delta}_r/\ddot{\delta}_o = 0.042$ is shown as Run No. 157 in Figure 24, and is very close to the curve from Eq. [8] .

Combining Eq. [1] with Eq. [8] gives:
$\ddot{\delta}_r = 0.036\ f(D_fF_v/m_f)^{0.5}(0.032)^r$, and for harmonic motion $\ddot{\delta} = \dot{\delta}(2\pi f)$ and $\delta_d = 2\dot{\delta}/2\pi f$. Therefore, three equations which represent soil motions under vibrating foundations for the soil tested are:

$$\ddot{\delta}_r = 0.036\ f(D_fF_v/m_f)^{0.5}(0.032)^r \qquad [9]$$

$$\dot{\delta}_r = (0.018/\pi)(D_fF_v/m_f)^{0.5}(0.032)^r \qquad [10]$$

$$(\delta_d)_r = (0.018/\pi^2 f)(D_fF_v/m_f)^{0.5}(0.032)^r \qquad [11]$$

Table 1. Test results for D_f = 6.28 in.

Run No.	W_f lbm	Y in.	R in.	F_m lbf	F_v lbf	f cps	A_d in.	A'_d in.	$\frac{\ddot{\delta}}{g} \times 10^4$	$\dot{\delta} \times 10^3$ ips	$\delta_d \times 10^5$ in.
1	6.02	7.75	0	62.1	10.4	42.0	0.22	0.53	415	60	47
2				60.7	12.9	29.6	0.15	0.72	208	42	45
3				60.3	15.1	22.4	0.15	0.94	160	43	62
4				60.1	17.0	17.1	0.14	1.23	114	41	78
5				60.1	20.0	10.1	0.15	1.99	75	45	143
6		7.75		60.2	22.2	5.5	0.19	3.32	57	64	366
7		5.83		60.3	10.4	41.8	0.22	0.53	415	60	46
8				59.6	13.1	29.6	0.17	0.72	236	48	52
9				59.6	15.4	22.2	0.16	0.95	169	46	66
10				59.3	17.5	17.0	0.14	1.23	114	41	76
11				59.4	20.2	10.1	0.08	1.99	40	24	76
12		5.83		59.4	22.3	5.5	0.08	3.34	24	27	156
13		3.90		60.9	10.6	41.4	0.35	0.54	649	96	75
14				60.4	13.1	30.2	0.26	0.71	366	75	80
15				60.4	15.5	22.2	0.22	0.95	232	64	86
16				60.4	17.6	17.3	0.17	1.21	141	51	94
17				60.9	20.5	10.2	0.12	1.98	61	37	114
18	6.02	3.90		60.7	22.4	5.5	0.11	3.33	33	37	214
19	7.40	2.20		60.3	10.6	40.8	0.28	0.54	519	78	61
20				60.4	13.1	30.2	0.14	0.71	197	40	42
21				60.5	15.9	22.3	0.09	0.94	96	25	35
22				60.4	17.8	17.1	0.15	1.23	122	44	81
23				60.5	20.5	10.2	0.40	1.97	203	122	380
24		2.20		60.5	22.5	5.5	0.66	3.33	198	221	1270
25		1.61		60.0	10.9	40.9	0.30	0.54	555	83	65
26				60.0	13.4	29.7	0.12	0.72	167	34	36
27				60.0	15.8	22.3	0.15	0.94	160	43	60
28				59.9	17.9	17.0	0.26	1.23	211	76	142
29				60.1	20.6	10.1	0.57	1.99	286	172	542
30	7.40	1.61	0	60.0	22.5	5.5	0.90	3.34	269	300	1730

Table 1. (continued)

Run No.	W_f lbm	Y in.	R in.	F_m lbf	F_v lbf	f cps	A_d in.	A'_d in.	$\frac{\ddot{\delta}}{g} \times 10^4$	$\dot{\delta} \times 10^3$ ips	$\delta_d \times 10^5$ in.
31	7.40	0.95	0	59.6	10.8	40.9	0.14	0.54	259	38	30
32				59.7	13.4	30.0	0.35	0.71	493	100	107
33				59.8	15.7	22.3	0.65	0.94	692	188	265
34				59.7	17.7	17.0	0.97	1.23	788	283	532
35				59.9	20.5	10.1	1.76	1.99	885	533	1685
36		0.95		59.8	22.5	5.5	2.77	3.34	830	930	5390
37		0.31		59.8	10.9	40.6	0.24	0.55	436	65	51
38				59.8	13.2	30.1	0.41	0.71	578	118	126
39				60.0	15.9	22.3	0.71	0.94	755	204	290
40				59.9	18.0	17.0	1.08	1.23	878	316	580
41				60.0	20.5	10.1	1.92	1.99	965	582	1840
42	7.40	0.31	0	60.1	22.5	5.5	3.01	3.34	900	1000	5800
43	6.02	7.90	4	60.9	10.7	41.6	0.10	0.53	189	28	22
44				60.9	13.5	29.4	0.08	0.72	111	23	24
45				61.1	15.9	22.3	0.07	0.94	75	20	28
46				61.2	18.0	17.0	0.05	1.23	41	15	27
47				61.2	20.6	10.1	0.09	1.99	45	27	85
48		7.90	4	61.3	22.6	5.5	0.12	3.34	36	40	231
49		7.95	8	61.2	11.0	40.7	0.07	0.55	127	19	15
50				61.3	13.5	30.1	0.05	0.71	71	14	15
51				61.3	16.0	22.3	0.06	0.94	64	17	24
52				61.5	18.0	17.2	0.06	1.22	49	18	33
53				61.4	20.7	10.1	0.05	1.99	25	15	49
54		7.95	8	61.5	22.5	5.5	0.07	3.34	21	23	135
55		8.03	12	60.4	10.9	41.2	0.08	0.54	148	22	18
56				60.1	13.7	29.5	0.04	0.72	56	11	12
57				60.2	16.0	22.2	0.06	0.95	63	16	23
58				60.3	18.1	17.0	0.06	1.23	49	18	33
59				60.2	20.7	10.2	0.05	1.97	25	15	49
60	6.02	8.03	12	60.3	22.5	5.5	0.04	3.33	12	13	78

Table 1. (continued)

Run No.	W_f lbm	Y in.	R in.	F_m lbf	F_v lbf	f cps	A_d in.	A'_d in.	$\frac{\ddot{\delta}}{g} \times 10^4$	$\dot{\delta} \times 10^3$ ips	$\delta_d \times 10^5$ in.
61	6.02	6.25	4	61.2	10.9	40.1	0.09	0.55	164	25	19
62				61.0	13.4	30.0	0.07	0.71	99	20	21
63				60.9	15.9	22.3	0.07	0.94	74	20	29
64				61.1	18.0	17.1	0.06	1.23	49	18	33
65				61.3	20.7	10.1	0.16	1.99	80	48	150
66		6.25		61.3	22.5	5.5	0.24	3.33	72	82	480
67		4.21		61.3	10.9	40.8	0.13	0.54	240	36	28
68				61.3	13.5	29.8	0.06	0.72	83	16	17
69				61.2	16.0	22.4	0.10	0.94	106	28	40
70				61.3	18.0	17.0	0.11	1.23	89	32	59
71				61.3	20.6	10.2	0.24	1.98	121	73	230
72	6.02	4.21		61.3	22.5	5.5	0.36	3.34	108	121	700
73	7.40	2.44		60.0	10.5	40.6	0.22	0.55	400	60	47
74					12.9	29.7	0.13	0.72	180	37	40
75					15.2	22.3	0.08	0.94	85	23	33
76					17.2	17.0	0.06	1.23	49	18	33
77					20.0	10.2	0.12	1.97	61	37	115
78		2.44		60.0	22.0	5.5	0.19	3.34	57	64	370
79		1.67		59.8	10.5	41.5	0.25	0.53	471	71	55
80				59.8	13.0	29.9	0.17	0.71	240	49	52
81				59.8	15.4	22.3	0.10	0.94	106	28	40
82				59.9	17.4	17.1	0.07	1.23	57	20	39
83				60.0	20.1	10.3	0.06	1.96	31	19	59
84		1.67	4	60.0	22.0	5.5	0.11	3.34	33	37	215
85		0.95	2	60.1	10.6	40.8	0.26	0.54	481	72	56
86				60.1	13.2	29.9	0.13	0.71	183	38	40
87				60.1	15.7	22.3	0.12	0.94	128	34	48
88				60.2	17.6	17.1	0.18	1.23	146	53	97
89				60.2	20.3	10.1	0.35	1.99	176	106	330
90	7.40	0.95	2	60.4	22.3	5.5	0.70	3.34	210	235	1350

Table 1. (continued)

Run No.	W_f lbm	Y in.	R in.	F_m lbf	F_v lbf	f cps	A_d in.	A'_d in.	$\frac{\ddot{\delta}}{g} \times 10^4$	$\dot{\delta} \times 10^3$ ips	$\delta_d \times 10^5$ in.
91	7.40	0.89	4	60.0	10.6	41.2	0.25	0.54	463	70	54
92				59.8	13.2	29.8	0.17	0.72	236	48	52
93				60.0	15.6	22.4	0.15	0.94	160	43	61
94				60.0	17.6	17.1	0.12	1.23	98	35	65
95				60.0	20.1	10.1	0.11	1.99	55	33	103
96		0.89		60.0	22.1	5.5	0.09	3.34	27	31	180
97		0.27		59.6	10.5	40.8	0.22	0.54	408	61	48
98				59.6	13.0	30.0	0.16	0.71	225	46	49
99				59.6	15.4	22.4	0.12	0.94	128	34	48
100				59.6	17.5	17.0	0.11	1.23	89	32	59
101				59.7	20.1	10.1	0.10	1.99	50	30	94
102		0.27	4	60.0	22.0	5.5	0.08	3.33	24	27	155
103		0.26	3	59.3	10.8	40.6	0.33	0.55	600	90	70
104				59.3	13.2	29.8	0.23	0.72	319	65	70
105				59.2	15.5	22.3	0.16	0.94	170	46	64
106				59.5	17.6	17.1	0.15	1.23	122	44	81
107				59.6	20.2	10.1	0.07	1.99	35	21	67
108			3	59.6	22.1	5.5	0.06	3.32	18	20	116
109			2	59.9	10.9	40.6	0.20	0.55	364	55	42
110				60.0	13.3	29.6	0.09	0.72	125	26	27
111					15.5	22.3	0.24	0.94	256	68	98
112					17.5	17.0	0.37	1.23	301	108	200
113					20.3	10.1	0.76	1.99	382	230	720
114		0.26	2		22.1	5.5	1.11	3.32	334	372	2150
115		0	0		10.7	41.0	0.40	0.54	741	111	87
116					13.2	29.8	0.76	0.72	1055	224	237
117					15.7	22.3	1.20	0.94	1280	351	490
118					17.7	17.1	1.65	1.23	1340	481	880
119					20.4	10.1	2.90	1.99	1460	882	2730
120	7.40	0	0	60.0	22.3	5.5	4.70	3.34	1410	1585	9200

Table 1. (continued)

Run No.	W_f lbm	Y in.	R in.	F_m lbf	F_v lbf	f cps	A_d in.	A'_d in.	$\frac{\ddot{\delta}}{g} \times 10^4$	$\dot{\delta} \times 10^3$ ips	$\delta_d \times 10^5$ in.
121	7.40	0	0	60.0	10.7	41.0	1.20	0.54	2222	335	260
122					13.2	29.8	1.30	0.72	1807	376	406
123					15.7	22.3	1.40	0.94	1490	405	560
124					17.7	17.1	1.60	1.23	1300	465	870
125					20.4	10.1	2.20	1.99	1106	670	2100
126		0			22.3	5.5	3.20	3.34	958	1060	6200
127		0.75			10.7	41.0	0.34	0.54	630	95	74
128					13.2	29.8	0.73	0.72	1013	217	230
129					15.7	22.3	1.20	0.94	1280	350	490
130					17.7	17.1	1.63	1.23	1325	478	880
131					20.4	10.1	2.78	1.99	1398	843	2600
132		0.75			22.3	5.5	4.60	3.34	1380	1540	8900
133		1.42			10.7	41.0	0.24	0.54	445	67	52
134					13.2	29.8	0.38	0.72	528	111	120
135					15.7	22.3	0.63	0.94	670	182	250
136					17.7	17.1	0.94	1.23	765	274	508
137					20.4	10.1	1.60	1.99	804	486	1520
138		1.42			22.3	5.5	2.53	3.34	758	840	4900
139		2.09			10.7	41.0	0.30	0.54	555	83	65
140					13.2	29.8	0.12	0.72	167	34	36
141					15.7	22.3	0.22	0.94	234	63	86
142					17.7	17.1	0.37	1.23	301	107	200
143					20.4	10.1	0.72	1.99	362	220	680
144		2.09			22.3	5.5	1.10	3.34	329	370	2110
145		2.62			10.7	41.0	0.32	0.54	593	89	69
146					13.2	29.8	0.18	0.72	250	51	54
147					15.7	22.3	0.10	0.94	106	29	40
148					17.7	17.1	0.15	1.23	122	44	81
149					20.4	10.1	0.35	1.99	176	105	330
150	7.40	2.62	0	60.0	22.3	5.5	0.56	3.34	168	187	1070

Table 1. (continued)

Run No.	W_f lbm	Y in.	R in.	F_m lbf	F_v lbf	f cps	A_d in.	A'_d in.	$\frac{\ddot{\delta}}{g} \times 10^4$	$\dot{\delta} \times 10^3$ ips	$\delta_d \times 10^5$ in.
151	7.40	3.31	0	60.0	10.7	41.0	0.30	0.54	555	83	65
152					13.2	29.8	0.19	0.72	264	54	57
153					15.7	22.3	0.11	0.94	117	31	43
154					17.7	17.1	0.09	1.23	73	26	48
155					20.4	10.1	0.22	1.99	111	67	220
156	7.40	3.31		60.0	22.3	5.5	0.37	3.34	111	123	720
157	6.02	8.40		61.3	21.9		0.04	1.99	20	22	130
158	6.02	6.51		61.2	22.2		0.05		25	28	162
159	6.02	4.52		61.1			0.11		55	61	355
160	7.40	3.01		59.7			0.16		80	89	520
161		1.97		59.1			0.35		176	196	1140
162		1.57		59.9			0.38		191	214	1240
163		1.18		59.4			0.35		176	196	1140
164		0.79		59.4			0.40		201	226	1300
165		0.39		59.8			0.69	1.99	346	385	2240
166		0		60.0			0.80	0.22	3640	4040	23300
167	7.40	0	0	59.3	22.2	5.5	0.35	0.22	1590	1770	10100

Table 2. Test results for D_f = 5 in.

Run No.	W_f lbm	Y in.	R in.	F_m lbf	F_v lbf	f cps	A_d in.	A'_d in.	$\frac{\ddot{\delta}}{g} \times 10^4$	$\dot{\delta} \times 10^3$ ips	$\delta_d \times 10^5$ in.
168	7.15	0	0	44.5	23.0	5.6	1.01	1.98	510	565	3300
169				42.3	20.5	10.3	0.72	1.55	464	277	880
170				40.0	22.5	17.4	0.39	1.20	325	115	215
171				37.5	15.5	23.0	0.24	1.01	238	63	87
172		0		30.0	13.0	30.4	0.29	0.83	349	71	75
173		2.08		24.3	7.8	5.6	0.08	1.98	40	44	260
174				43.5	15.5	5.6	0.12	1.98	61	68	395
175				48.3	22.8	5.6	0.35	1.98	177	196	1140
176				24.3	7.3	10.3	0.09	1.55	58	35	110
177				43.5	14.0	10.3	0.18	1.55	116	70	220
178				46.5	21.0	10.3	0.29	1.55	187	112	350
179				24.3	6.3	17.5	0.14	1.20	117	41	76
180				43.3	12.3	17.4	0.22	1.20	183	66	121
181				43.5	18.0	17.5	0.30	1.20	250	90	167
182				24.0	5.5	22.9	0.20	1.01	198	53	73
183				43.3	10.8	23.1	0.27	1.01	267	71	98
184				41.5	16.0	22.5	0.46	1.02	451	122	166
185				24.0	4.5	30.4	0.21	0.83	253	52	55
186				43.0	9.0	30.1	0.31	0.83	374	76	81
187		2.08	0	38.5	13.5	30.0	0.52	0.83	627	130	142
188		1.98	4	24.1	7.8	5.6	0.05	1.98	25	28	163
189				42.0	15.1	5.6	0.07	1.98	35	39	230
190				48.0	22.2	5.6	0.08	1.98	40	44	260
191				24.0	7.0	10.3	0.07	1.55	45	27	84
192				42.0	13.8	10.2	0.09	1.55	58	35	110
193				46.0	20.1	10.3	0.12	1.55	77	46	145
194				41.9	11.8	17.4	0.14	1.20	117	42	77
195				43.7	17.1	17.4	0.15	1.20	125	45	83
196				41.7	10.4	23.4	0.12	1.00	120	32	44
197				41.2	14.8	22.9	0.16	1.01	158	42	58
198				41.7	8.7	30.3	0.13	0.83	157	32	34
199	7.15	1.98	4	46.3	12.7	30.3	0.19	0.83	229	46	49

Table 3. Test results for D_f = 6 in.

Run No.	W_f lbm	Y in.	R in.	F_m lbf	F_v lbf	f cps	A_d in.	A'_d in.	$\frac{\ddot{\delta}}{g} \times 10^4$	$\dot{\delta} \times 10^3$ ips	$\delta_d \times 10^5$ in.
200	7.28	0	0	22.0	8.0	5.6	0.30	1.98	152	169	980
201				42.0	15.5	5.6	0.60	1.98	303	335	1950
202				49.0	22.5	5.6	0.91	1.98	460	508	3000
203				21.5	7.0	10.3	0.22	1.55	142	86	265
204				41.5	14.0	10.2	0.46	1.56	295	179	560
205				48.0	20.5	10.3	0.70	1.55	452	273	860
206				21.5	6.0	17.6	0.12	1.20	100	35	65
207				41.5	12.0	17.2	0.26	1.21	215	77	141
208				46.5	17.5	17.4	0.38	1.20	316	114	210
209				22.0	5.8	22.9	0.10	1.01	99	26	36
210				41.5	10.5	22.6	0.16	1.02	157	43	58
211				45.5	15.5	22.9	0.22	1.01	218	58	80
212		0		44.0	13.3	29.5	0.18	0.84	214	44	46
213		2.21		24.5	8.0	5.6	0.12	1.98	61	68	395
214				42.0	15.5	5.6	0.21	1.98	106	117	680
215				50.8	23.3	5.6	0.31	1.98	157	174	1010
216				24.3	7.3	10.3	0.14	1.55	90	54	170
217				41.8	14.3	10.2	0.25	1.56	160	96	300
218				49.8	21.3	10.3	0.35	1.55	226	136	420
219				24.5	6.0	17.5	0.19	1.20	158	57	104
220				41.8	12.3	17.2	0.30	1.21	248	89	164
221				49.0	18.5	17.5	0.43	1.20	358	122	225
222				24.5	6.0	22.9	0.22	1.01	218	58	80
223				41.5	11.0	22.3	0.34	1.03	330	89	122
224				48.3	16.3	22.8	0.46	1.01	455	122	169
225				24.3	4.8	29.8	0.25	0.84	298	61	64
226				41.8	9.3	30.1	0.42	0.83	506	103	110
227		2.21		47.3	13.8	30.2	0.52	0.83	627	130	140
228		5.40		34.0	7.5	5.6	0.07	1.98	35	39	228
229	7.28	5.40	0	54.0	15.0	5.6	0.10	1.98	51	57	330

Table 3. (continued)

Run No.	W_f lbm	Y in.	R in.	F_m lbf	F_v lbf	f cps	A_d in.	A'_d in.	$\frac{\ddot{\delta}}{g} \times 10^4$	$\dot{\delta} \times 10^3$ ips	$\delta_d \times 10^5$ in.
230	7.28	5.40	0	59.5	22.0	5.6	0.13	1.98	66	73	425
231				34.0	7.0	10.3	0.10	1.55	65	39	123
232				54.0	13.5	10.4	0.13	1.55	84	50	160
233				59.5	20.0	10.3	0.18	1.55	116	70	220
234				34.0	6.0	17.4	0.12	1.20	100	35	65
235				54.0	11.5	17.6	0.16	1.19	134	48	88
236				59.3	17.3	17.4	0.25	1.20	208	74	138
237				34.0	5.0	22.9	0.11	1.01	109	29	40
238				54.0	10.5	22.6	0.18	1.02	176	47	65
239				59.0	15.5	22.8	0.26	1.01	258	69	95
240				34.0	4.5	30.3	0.13	0.83	157	32	34
241				54.0	9.0	29.9	0.22	0.84	262	53	56
242				59.0	13.0	30.5	0.27	0.82	329	67	71
243				34.0	3.8	42.7	0.14	0.65	216	32	25
244				54.0	7.5	41.8	0.28	0.66	424	64	50
245	7.28	5.40		58.8	11.3	42.4	0.41	0.65	631	91	68
246	5.90	9.54		21.8	7.5	5.6	0.08	1.49	54	60	350
247				42.6	14.8	5.6	0.07	1.49	47	52	305
248				60.3	22.5	5.6	0.15	1.49	101	113	650
249				21.8	7.0	10.3	0.09	1.26	71	43	133
250				42.5	13.8	10.3	0.12	1.26	95	57	180
251				60.6	20.3	10.3	0.14	1.26	111	67	210
252				21.8	5.8	17.1	0.10	1.03	97	35	65
253				42.6	11.8	17.5	0.14	1.02	137	49	90
254				60.3	17.5	17.4	0.19	1.02	186	67	123
255				21.8	5.0	22.6	0.09	0.91	91	24	33
256				42.3	10.0	22.7	0.13	0.91	131	35	48
257				60.1	15.3	22.8	0.17	0.91	172	46	64
258				21.8	4.5	30.2	0.12	0.79	152	31	33
259	5.90	9.54	0	42.5	8.8	29.7	0.14	0.80	175	36	38

Table 3. (continued)

Run No.	W_f lbm	Y in.	R in.	F_m lbf	F_v lbf	f cps	A_d in.	A'_d in.	$\frac{\ddot{\delta}}{g} \times 10^4$	$\dot{\delta} \times 10^3$ ips	$\delta_d \times 10^5$ in.
260	5.90	9.54	0	59.8	13.0	30.6	0.20	0.79	253	52	55
261	5.90	9.54	0	42.3	7.0	41.5	0.20	0.66	303	46	37
262	5.90	9.54	0	59.3	10.5	42.0	0.23	0.65	354	53	41
263	7.28	2.11	4	41.8	15.3	5.5	0.07	1.99	35	39	226
264				51.0	22.5	5.6	0.08	1.98	40	44	260
265				41.6	13.8	10.2	0.09	1.55	58	35	110
266				50.0	20.5	10.3	0.10	1.55	65	39	124
267				41.5	11.5	17.4	0.13	1.20	108	38	71
268				48.8	17.3	17.3	0.15	1.20	125	45	83
269				41.5	10.3	22.9	0.14	1.01	139	37	51
270				47.8	15.3	23.0	0.18	1.01	178	47	65
271				41.5	8.5	30.2	0.17	0.83	205	41	44
272	7.28	2.11	4	46.2	13.0	30.2	0.22	0.83	267	54	57
273	4.57	15.00	0	72.7	22.5	5.5	0.15	1.99	75	84	480
274	4.57	14.03		73.7	23.5		0.15		75	84	480
275	4.57	12.80		72.7	23.0		0.16		80	89	515
276	4.91	11.62		73.8	24.0		0.17		85	95	550
277	4.91	10.50		72.3	23.0		0.17		85	95	550
278	5.90	9.22		71.8			0.17		85	95	550
279		8.12		71.5			0.19		95	106	610
280		6.95		71.5			0.21		105	118	680
281		5.76		71.3			0.24		120	133	760
282	5.90	4.64		71.3	23.0		0.21		105	118	680
283	7.28	3.48		70.3	22.8		0.29		145	162	940
284		2.28		70.0	23.0		0.16	1.99	80	89	515
285		0.95		69.8	22.8		1.09	0.19	5730	6400	37100
286		0		69.3	22.7		0.60	1.99	300	335	1940
287		0		69.0	22.8		1.16		580	648	3800
288		0.65		69.3	22.7		0.38		190	211	1220
289		1.83		70.0	22.8		0.12		60	67	385
290	7.28	2.89	0	68.7	22.7	5.5	0.08	1.99	40	44	260

Table 4. Test results for D_f = 7 in.

Run No.	W_f lbm	Y in.	R in.	F_m lbf	F_v lbf	f cps	A_d in.	A'_d in.	$\frac{\ddot{\delta}}{g} \times 10^4$	$\dot{\delta} \times 10^3$ ips	$\delta_d \times 10^5$ in.
291	7.42	0	0	23.2	7.6	5.6	0.26	1.98	131	147	850
292				40.0	15.5	5.6	0.56	1.98	283	314	1840
293				42.5	22.5	5.6	0.92	1.98	465	520	3000
294				23.5	7.0	10.3	0.22	1.55	142	86	270
295				40.0	14.0	10.3	0.46	1.55	297	179	560
296				42.0	20.5	10.3	0.68	1.55	438	264	830
297				23.3	5.8	17.4	0.11	1.20	91	33	61
298				40.0	12.0	17.1	0.25	1.22	205	74	135
299				40.5	17.5	17.2	0.40	1.21	331	119	220
300				23.5	5.0	23.0	0.06	1.01	59	16	21
301				40.0	10.5	22.8	0.17	1.01	167	44	61
302				38.8	15.3	22.9	0.23	1.01	228	61	84
303		0		38.0	12.5	30.3	0.18	0.83	217	44	46
304		2.30		23.8	8.0	5.6	0.10	1.98	51	57	330
305				42.5	16.0	5.6	0.19	1.98	96	107	620
306				51.8	23.3	5.6	0.42	1.98	212	236	1380
307				23.8	7.3	10.3	0.13	1.55	84	50	160
308				42.5	14.5	10.3	0.22	1.55	142	85	265
309				51.0	21.0	10.4	0.44	1.55	284	170	535
310				23.8	6.3	17.4	0.15	1.20	125	45	83
311				42.3	12.3	17.5	0.28	1.20	233	83	154
312				50.0	18.0	17.5	0.43	1.20	358	127	235
313				23.5	5.5	22.8	0.18	1.01	178	47	65
314				42.1	10.9	22.9	0.31	1.01	307	82	112
315				49.3	16.0	23.1	0.48	1.01	475	126	176
316				23.6	4.6	30.4	0.21	0.83	253	52	55
317				41.8	9.3	30.3	0.34	0.83	410	84	91
318		2.30		48.5	13.5	30.6	0.53	0.82	647	130	140
319		5.50		23.3	7.8	5.6	0.10	1.98	51	57	330
320	7.42	5.50	0	42.0	15.5	5.6	0.16	1.98	81	90	525

Table 4. (continued)

Run No.	W_f lbm	Y in.	R in.	F_m lbf	F_v lbf	f cps	A_d in.	A'_d in.	$\frac{\ddot{\delta}}{g} \times 10^4$	$\dot{\delta} \times 10^3$ ips	$\delta_d \times 10^5$ in.
321	7.42	5.50	0	49.8	22.8	5.6	0.21	1.98	106	117	680
322				23.3	7.3	10.4	0.11	1.55	71	43	134
323				42.0	14.0	10.3	0.18	1.55	116	70	220
324				49.8	20.8	10.3	0.22	1.55	142	85	265
325				23.0	6.0	17.5	0.11	1.20	92	33	62
326				42.0	12.0	17.5	0.22	1.20	183	66	120
327				49.5	18.0	17.4	0.29	1.20	241	86	160
328				23.0	5.5	22.9	0.11	1.01	109	29	40
329				42.0	10.8	23.0	0.20	1.01	198	53	72
330				49.8	15.8	22.9	0.28	1.01	277	74	102
331				23.0	4.5	30.3	0.13	0.83	157	32	34
332				42.0	9.0	30.3	0.23	0.83	277	56	59
333				49.5	13.3	30.1	0.29	0.83	350	71	76
334				23.0	3.5	42.0	0.18	0.65	278	42	33
335				42.0	7.5	41.6	0.29	0.66	429	64	50
336	7.42	5.50		49.3	10.8	41.5	0.42	0.66	636	95	74
337	6.05	9.66		25.1	7.8	5.6	0.07	1.49	47	53	305
338				44.8	15.0	5.6	0.12	1.49	81	90	525
339				61.3	22.5	5.6	0.12	1.49	81	90	525
340				24.8	7.0	10.3	0.08	1.26	63	38	120
341				45.1	13.8	10.3	0.11	1.25	88	53	165
342				61.3	20.0	10.3	0.12	1.26	95	57	180
343				25.3	6.0	17.3	0.06	1.03	58	21	39
344				45.1	11.8	17.5	0.10	1.02	98	35	65
345				61.3	17.5	17.3	0.19	1.03	184	66	120
346				24.8	5.0	22.7	0.07	0.91	77	20	28
347				44.8	10.0	22.8	0.11	0.91	121	32	45
348				61.3	15.5	22.6	0.14	0.91	154	41	57
349				25.1	4.3	30.5	0.07	0.79	89	18	19
350	6.05	9.66	0	44.9	8.6	30.3	0.15	0.79	190	39	41

Table 4. (continued)

Run No.	W_f lbm	Y in.	R in.	F_m lbf	F_v lbf	f cps	A_d in.	A'_d in.	$\frac{\ddot{\delta}}{g} \times 10^4$	$\dot{\delta} \times 10^3$ ips	$\delta_d \times 10^5$ in.
351	6.05	9.66	0	60.8	13.0	30.5	0.19	0.79	241	49	52
352				25.1	3.5	42.4	0.07	0.65	108	16	12
353				44.8	7.0	41.6	0.16	0.66	242	36	28
354	6.05	9.66	0	60.6	10.8	41.5	0.23	0.66	348	52	41
355	7.42	2.24	4	44.3	22.3	5.6	0.10	1.98	51	57	330
356				24.0	7.0	10.3	0.06	1.55	39	23	73
357				41.0	13.5	10.3	0.10	1.55	65	39	123
358				49.5	20.0	10.2	0.11	1.55	71	43	133
359				48.8	17.3	17.4	0.15	1.20	125	45	83
360				48.0	15.0	22.9	0.19	1.01	188	50	70
361	7.42	2.24	4	47.5	13.0	30.3	0.22	0.83	267	54	57
362	6.05	9.73	8	21.5	6.5	12.6	0.13	1.17	111	54	135
363			16	21.5	6.5	12.6	0.04		34	17	42
364			8	42.5	13.5	12.6	0.16		137	67	168
365			16	42.5	13.5	12.6	0.09		77	37	94
366			8	57.5	20.5	12.6	0.25		214	104	26
367	6.05	9.73	16	59.0	20.0	12.6	0.15	1.17	128	62	16

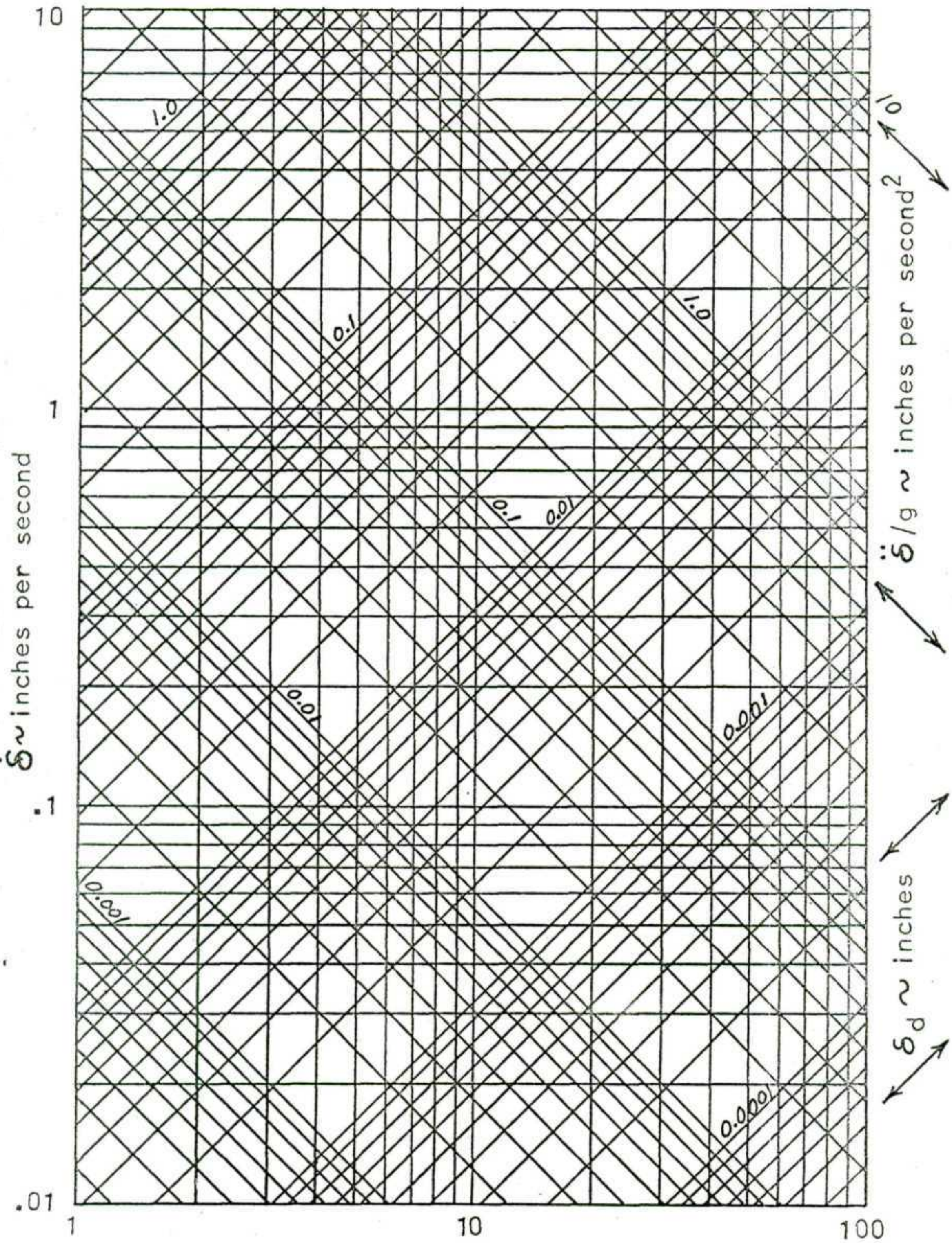

Figure 22. Vibration nomograph.

Table 5. Foundation settlements.

Run Nos. inclusive	H cm	H_b cm	S cm
1 - 6	60.00	58.50	1.50
7 - 12	55.00	53.60	1.40
13 - 18	50.00	48.70	1.30
19 - 24	45.00	44.30	0.70
25 - 30	43.00	42.75	0.25
31 - 36	41.00	40.70	0.30
37 - 42	39.00	38.80	0.20
43 - 48	60.00	58.30	1.70
49 - 54	60.00	58.40	1.60
55 - 60	60.00	58.60	1.40
61 - 66	55.00	54.10	0.90
67 - 72	50.00	48.90	1.10
73 - 78	45.00	44.40	0.60
79 - 84	43.00	42.45	0.55
85 - 90	41.00	40.60	0.40
91 - 96	41.00	40.45	0.55
97 - 102	39.00	38.90	0.10
103 - 108	39.00	38.85	0.15
109 - 114	39.00	38.85	0.15
157	60.00	59.35	0.65
158	55.00	54.55	0.45
159	50.00	49.50	0.50
160	46.00	45.65	0.35
161	43.00	42.70	0.30
162	42.00	41.75	0.25
163	41.00	40.80	0.20
164	40.00	39.80	0.20
165	39.00	38.80	0.20

Table 6.

Calibration curve and run correspondence.

Run Nos. inclusive	C_c
1 - 156	A
157 - 165	B
166 - 167	none *
168 - 245	B
246 - 262	C
263 - 284	B
285	none *
286 - 336	B
337 - 354	C
355 - 361	B
362 - 367	C

* Calibration was made immediately after run.

The difference between curves A, B, and C, was due to the electrical setup (Appendix D) and to the discharge of the batteries (Figure 15).

Table 7. Dimensionless values.

Run No.	$\frac{\ddot{\delta} m_f}{F_v}$	$\frac{f^2 D_f m_f}{F_v}$	$\frac{Y}{D_f}$	Key for Figure 23
121	0.154	18.90	0	
122	0.102	8.10		
123	0.070	3.80		
124	0.054	2.00		
125	0.040	0.60		
126	0.032	0.16	0	
214	0.0050	0.23	0.37	
215	0.0049	0.15		
217	0.0081	0.82		
218	0.0077	0.56		
220	0.0147	2.72		
221	0.0141	1.87		
222	0.0264	9.88		
223	0.0218	5.11		
224	0.0203	3.61		
225	0.0452	20.90		
227	0.0331	7.46	0.37	
319	0.0049	0.54	0.78	
320	0.0039	0.27		
321	0.0035	0.19		
322	0.0072	1.99		
323	0.0062	1.02		
324	0.0051	0.69		
326	0.0113	3.43		
327	0.0099	2.26		
329	0.0136	6.59		
330	0.0130	4.46		
331	0.0259	27.20		
332	0.0228	13.60		
333	0.0195	9.15		
334	0.0590	67.80	0.78	
339	0.0022	0.15	1.38	
340	0.0055	1.66		
341	0.0039	0.84		
342	0.0029	0.58		
343	0.0059	5.47		
344	0.0050	2.84		
346	0.0093	11.30		
347	0.0073	5.71		
348	0.0060	3.61		
349	0.0125	23.70		
350	0.0134	11.70		
351	0.0112	7.85		
353	0.0209	27.10	1.38	

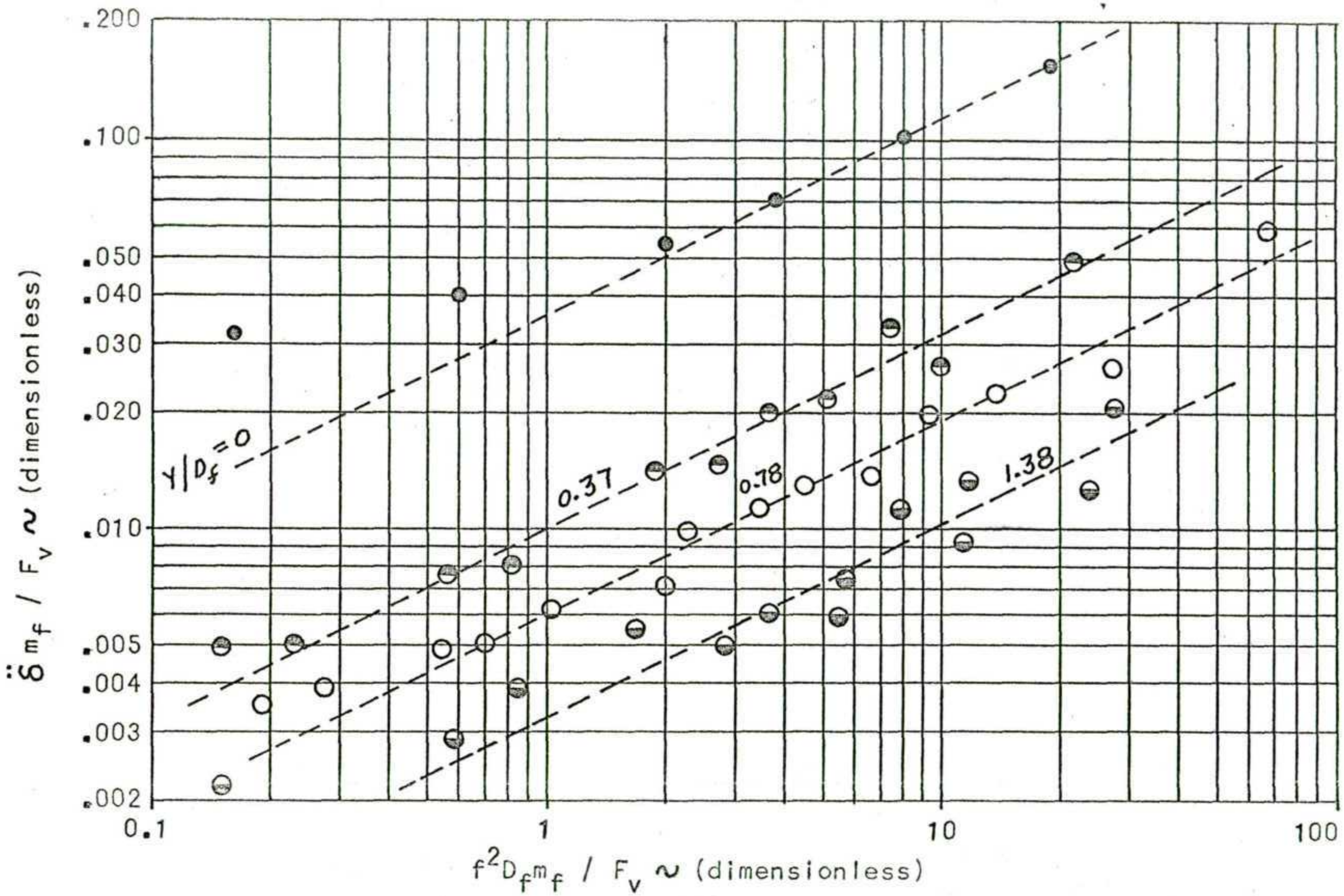

Figure 23. Logarithmic graph of values from Table 7.

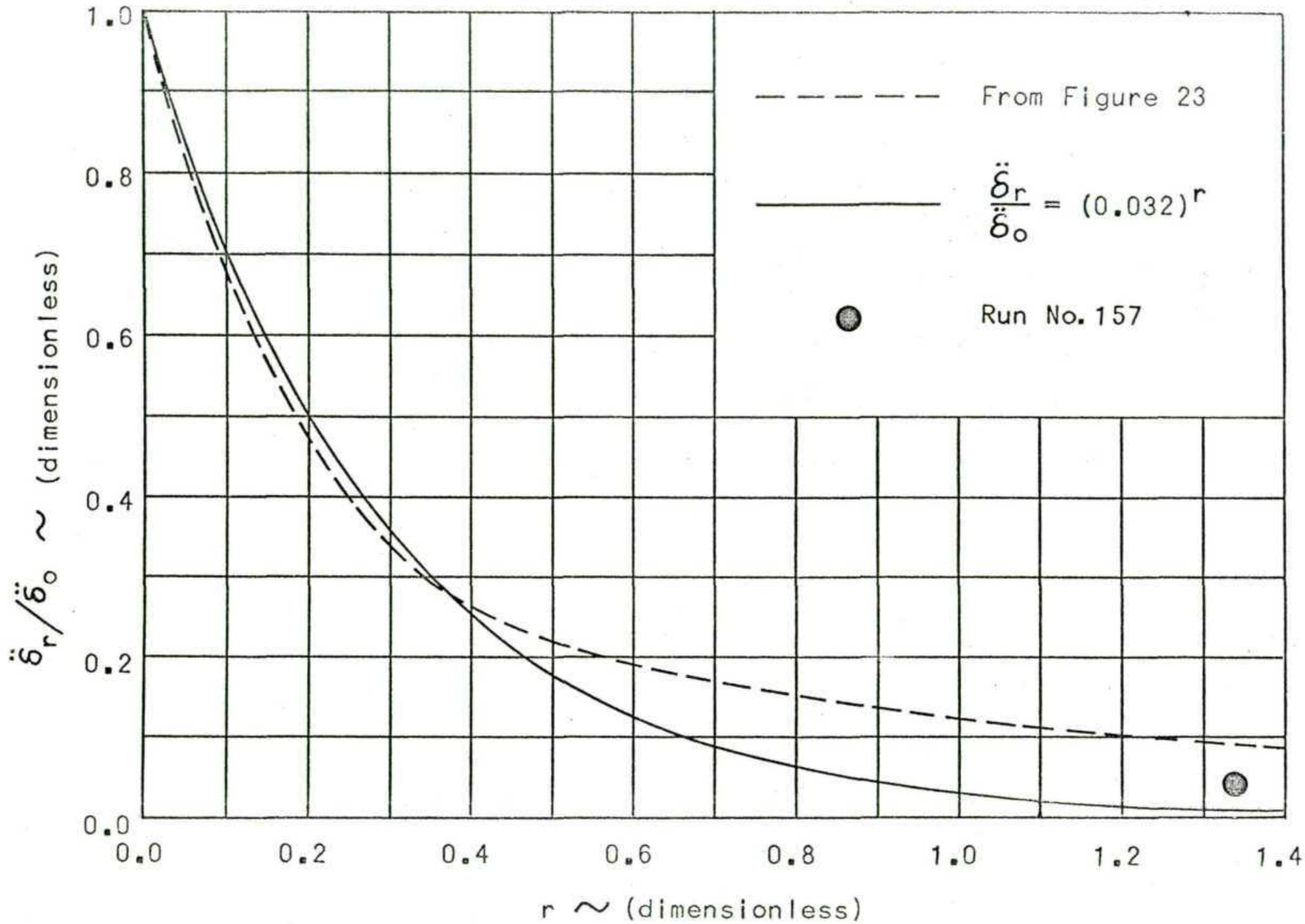

Figure 24. Graph of $\ddot{\delta}_r/\ddot{\delta}_o$ versus r, from Figure 23 and Equation 8.

CHAPTER V

CONCLUSIONS

The steady state soil motions, for standard 20 - 30 Ottawa sand, under vibrating foundations are represented by Equations [9] , [10], and [11] . These equations give values for maximum acceleration, velocity, and displacement, respectively.

The best technique for placing the accelerometer in the sand was; on a piece of filter paper and in contact with the bottom of the foundation when the motion of the foundation is desired, and supported only by the sand when motion of the sand is to be found.

Applying a kinetic energy approach to determine the mass of soil that vibrates with a foundation (Chapter I), and neglecting soil motion as a function of R, this gives kinetic energy = αY, where $\alpha = \frac{1}{2}(81 \rho D_f{}^3 F_v / g m_f \pi) \times 10^{-6}$, for $r = 0$. The differential kinetic energy at Y is $\alpha(0.032)^{2r}$ dY, and the total of the soil is $\int_0^{\infty} \alpha(0.032)^{2r} dY$. Remembering that $r = Y/D_f$, the integration gives $\alpha D_f/6.88$. Therefore, $Y = r_o/3.44$ and agrees rather closely with the theoretical, $Y = r_o/\pi$ from Chapter I.

CHAPTER VI

RECOMMENDATIONS

This investigation should be continued to include different soils and different soil properties. A 330-ohm resistor placed in series with the primary of the transformer (Figure 15) will give better response to low frequencies(9). This should be done before additional studies are made with the experimental equipment.

Further investigations should include the following:

1. Different instrumentation techniques.

2. Comparison of laboratory results with those of an actual soil-foundation system.

3. Determining the phase angle and soil motion relationships of a system.

4. Studies similar to this using miniature soil strain gages under development by United ElectroDynamics.

5. Experimentation with frequencies below 5 cps and above 50 cps, also in the vicinity of a soil-foundation system's natural frequency.

6. The effect of foundation vibrations on adjacent foundations.

7. The effects of using different shaped footings.

8. Dynamic loading of pile type foundations.

9. Systems having dynamic loads acting along three orthogonal axes and dynamic couples acting in the three planes formed by these axes.

10. Detailed analysis of oscillograph records at frequencies in 5 and with the film speed set at about 50 in. per sec. This speed would aid the study of phase angles.

REFERENCES

1. Symposium on Dynamic Testing of Soils, ASTM Special Technical Publication No. 156, American Society for Testing and Materials, Philadelphia 3, Pa., 1953.

2. Richart, F.E.,Jr., Foundation Vibrations, University of Florida Technical Paper No. 192, Gainsville, Fla., Oct 1960, p 9.

3. Allnutt, R.B., Mintz, F., Ormondroyd, J., and Specht, R.D., "Motion Measurements," Handbook of Experimental Stress Analysis, John Wiley and Sons, Inc., New York, N. Y., 1950, pp 301-389.

4. Ibid., Langer, B.F., "Electrical Inductance Gages," pp 238-300.

5. Ibid., Meier, J.H., "Strain Rosettes," pp 390-437.

6. The Aluminum Data Book, Reynolds Metals Co., Richmond 18, Va., 1958, pp 41 and 91.

7. Specifications and Instructions for Accelerometer Model 2221C, Endevco Corp., Pasadena, Calif., 1960.

8. Model 2614B Amplifier Instruction Manual, Endevco Corp., Pasadena, Calif., 1961.

9. Specifications and Instruction Manual for 2609.1 Transformer, Endevco Corp., Pasadena, Calif., 1961.

10. ASTM C190-59, "Standard Method of Test for Tensile Strength of Hydraulic Cement Mortars," ASTM Standards Part 4, American Society for Testing and Materials, Philadelphia 3, Pa., 1961, pp 196-197.

11. Taylor, D.W., Fundamentals of Soil Mechanics, John Wiley and Sons, Inc., New York, N. Y., 1954.

12. Werner, R.R., A Study of Poisson's Ratio and the Elastic and Plastic Properties of Ottawa Sand, a thesis at Texas A and M College, 1957.

13. Oldenburger, R., Mathematical Engineering Analysis, The Macmillian Co., New York, N. Y., 1950, pp 60-65.

14. ASTM D653-60, "Standard Definitions of Terms and Symbols Relating to Soil Mechanics," <u>ASTM Standards Part 4</u>, American Society for Testing and Materials, Philadelphia 3, Pa., 1961, pp 1402-1419.

15. Ibid., ASTM D1707-60T,"Tentative Definitions of Terms Relating to Soil Dynamics," pp 1396-1401.

16. Terzaghi, Karl and Peck, R.B., <u>Soil Mechanics in Engineering Practice</u>, John Wiley and Sons, Inc., New York, N. Y., 1948, pp 111-113.

17. Terzaghi, Karl, <u>Theoretical Soil Mechanics</u>, John Wiley and Sons, Inc., New York, N. Y., 8th Printing, August 1956, pp 434-479.

APPENDIX A

Force Gage Calibration (Figures 3, 4, and 13)

Compression test with loading rod zeroed out.

(microinches / inch)

Load	Loading			Unloading		
lbm	1st	2nd	3rd	1st	2nd	3rd
0	7750	7760	7760	7760	7765	7765
10	7880	7890	7890	7890	7895	7890
20	8010	8015	8015	8015	8020	8020
30	8140	8145	8145	8150	8150	8150
40	8270	8280	8275	8280	8285	8280
50	8405	8410	8410	8410	8415	8410
60	8535	8540	8540	8540	8545	8540
70	8670	8670	8670	8670	8675	8670
80	8800	8805	8800	8805	8805	8805
90	8935	8930	8930	8935	8940	8935
100	9065	9065	9065	9065	9065	9065

Average is 13.05 microinches / inch-pound

Spring Calibration (Figure 5)

Spring	Follower Position	Indicator (μ in/in)	Change (μ in/in)	Force (lbf)	k (lbf/in)
Gold	up	7885			
	down	8110	225	17.24	51.62
	up	7885	225	17.24	51.62
	down	8110	225	17.24	51.62
Gold	up	7885	225	17.24	51.62
Black	up	7880			
	down	8105	225	17.24	51.62
	up	7880	225	17.24	51.62
	down	8105	225	17.24	51.62
Black	up	7880	225	17.24	51.62
Clear	up	7875			
	down	8105	230	17.62	52.75
	up	7875	230	17.62	52.75
	down	8105	230	17.62	52.75
Clear	up	7875	230	17.62	52.75
All	up	8130			
	down	8810	680	52.11	156.0
	up	8130	680	52.11	156.0
	down	8810	680	52.11	156.0
All	up	8130	680	52.11	156.0

APPENDIX B

Endevco Accelerometer

Type VI Piezite® element

Model 2221C, Serial EB 12

Sensitivity in (peak mv/peak g), $E_s = 14.0$ *

Sensitivity in (RMS mv/peak g), $E_c = 9.90$ *

Accelerometer capacity in pf, $C_p = 686$

Sensitivity in (peak ρ coulombs/peak g),

$E_s(C_p + 300) \times 10^{-3} = 13.8$

Maximum transverse sensitivity = 3.3%

Frequency, (cps)	Deviation, (%)
20	-1.0
50	0.0
100	+1.0
200	+1.0
400	+1.0
1000	+1.0
2000	+1.0
4000	+1.0

* 300 pf total external capacity added for all sensitivity calibrations

Standardization of accelerometer to E = 8 RMS mv/peak g:

$$C_t = (E_c/E)(C_p + C_{cal}) - C_p$$

$$C_t = (9.90/8.00)(686 + 300) - 686 = 534\ \mu\mu f$$

318 $\mu\mu$f, 10 ft cable (factory tagged)
30 $\mu\mu$f, residual amplifier capacity
91 $\mu\mu$f, 3 ft cable (factory tagged)
5 $\mu\mu$f, Tee box (assumed)
444 $\mu\mu$f

534 - 444 = 90 $\mu\mu$f, added to step capacity adjustment in amplifier.

APPENDIX C

Sand Weight

W ~ lbm	H ~ cm	W/H ~ lbm/cm
1411	38.5	36.66
1614	44.0	36.69
1916	52.1	36.77
2319	63.2	36.70
2826	77.0	36.71

Average is 36.71 lbm/cm

Weights of Soil Loading Parts

Part			Grams
Follower with bearings			222.7
Springs:	Gold		13.5
	Black		13.2
	Clear		13.2
Loading bar with bearings and adapter			393.3
Column Adapter			166.6
Columns:	Long		1294.7
	Intermediate		978.0
	Short		525.3
Locking nut			52.1
Threaded rods:		Long	834.2
		Intermediate	526.7
		Short	371.8
Force transducer with lead wire supported			130.0
Force transducer adapter			165.8
Plywood disk with steel loading plate:			
	5 inch diameter		205.3
	6 inch diameter		267.3
	6.28 inch diameter		319.9
	7 inch diameter		329.0

APPENDIX D

Accelerometer Placement

Run Nos. inclusive	Method Used
1 - 114	On filter paper
115 - 120	Screwed to foundation
121 - 156	On filter paper
157 - 166	In sand only
167	Screwed to foundation
168 - 172	Screwed on fiber washer to foundation
173 - 199	Slipped over insulated rod
200 - 212	Screwed on fiber washer to foundation
213 - 285	Slipped over insulated rod
286	Screwed on fiber washer to foundation
287	Screwed to foundation
288 - 290	Screwed to aluminum disk, 3 in. in dia.
291 - 303	Screwed on fiber washer to foundation
304 - 367	Slipped over insulated rod

Electrical Information

Run Nos. inclusive	C_c	Galvanometer Used	Oscillograph Channel	Amplifier Gain
1 - 156	A	X9970	7	3
157 - 165	B	X6797	2	10
166 - 167	none	X6797	2	1
168 - 284	B,C	X6797	2	10
285	none	X6797	2	1
286 - 367	B,C	X6797	2	10

APPENDIX E

Determining the Foundation Mass (Table 1 and Figure 12)

For Runs 1 through 18:

Loading bar with bearings and adapter	393.3	gms
Column adapter	166.6	gms
Column, intermediate	978.0	gms
Locking nut	52.1	gms
Threaded rod, intermediate	526.7	gms
W_a =	2116.7	gms
Force transducer/lead wire supported	130.0	gms
Force transducer adapter	165.8	gms
6.28 in. dia. disk/steel plate	319.9	gms
W_b =	615.7	gms

$W_f = W_a + W_b = 2732.4$ gms $= 6.02$ lbm

For Runs 19 through 42:

Loading bar with bearings and adapter	393.3	gms
Column adapter	166.6	gms
Column, long	1294.7	gms
Locking nut	52.1	gms
Threaded rod, long	834.2	gms
W_a =	2740.9	gms

No change in W_b

$W_f = 3356.6$ gms $= 7.40$ lbm

Determining F_m for Run No. 291 (Table 4 and Figure 20)

$F_m = (F_1 + F_2)/(2) - W_a$

$F_m = (21.6 + 36.8)/(2) - 6.0$

$F_m = 23.2$ lbf